Climate change and elevated CO₂ favor forest over savanna under different future scenarios in South Asia

Dushyant Kumar[1], Mirjam Pfeiffer[1], Camille Gaillard[1], Liam Langan[1], and Simon Scheiter[1]

[1]Senckenberg Biodiversity and Climate Research Centre (SBiK-F), Senckenberganlage 25, 60325 Frankfurt am Main, Germany

Correspondence: Dushyant Kumar (dushyant.kumar@senckenberg.de)

Abstract.

South Asian vegetation provides essential ecosystem services to the region and its 1.7 billion inhabitants that are closely linked to its land-use forms and carbon storage potential. Yet, biodiversity is threatened by climate and land-use change. Understanding and assessing how ecosystems respond to simultaneous increases in atmospheric CO₂ and future climate change is of vital importance to avoid undesired ecosystem change. A failure to react to increasing CO₂ and climate change will likely have severe consequences for biodiversity and humankind. Here, we used the aDGVM2 to simulate vegetation dynamics in South Asia under RCP4.5 and RCP8.5, and we explored how the presence or absence of CO₂ fertilization influences vegetation responses to climate change. Simulated vegetation under both RCPs without CO₂ fertilization effects showed decrease in tree dominance and biomass, whereas simulations with CO₂ fertilization showed an increase in biomass, canopy cover, and tree height and a decrease in biome-specific evapotranspiration by the end of the 21st century. The model predicted changes in above ground biomass and canopy cover that trigger biome transition towards tree-dominated systems. We found that savanna regions are at high risk of woody encroachment and transitioning into forest. We also found transitions of deciduous forest to evergreen forest in the mountain regions. C₃ photosynthesis dependent vegetation was not saturated at current CO₂ concentrations and the model simulated a strong CO₂ fertilization effect with the rising CO₂. Hence, vegetation in the region will likely remain a carbon sink. Projections showed that the bioclimatic envelopes of biomes need adjustments to account for shifts caused by climate change and eCO₂. The results of our study help to understand the regional climate-vegetation interactions and can support the development of regional strategies to preserve ecosystem services and biodiversity under elevated CO₂ and climate change.

1   Introduction

Global climate has been identified as the primary determinant of large-scale natural vegetation patterns (Overpeck et al., 1990). Climate change has affected global vegetation pattern in the past and caused numerous shifts in plant species distribution over

the last few decades (Chen et al., 2011; Thuiller et al., 2008). It is expected to have even more pronounced effects in the future that may lead to drastically increasing species extinction rates in various ecosystems (Brodie et al., 2014). Natural ecosystems

25 have been and continue to be exposed to increased climate variability and abrupt changes caused by increased intensity and frequency of extreme events such as heat waves, drought and flooding (Herring et al., 2018). At the same time, they are under severe pressure due to anthropogenic disturbance and land conversion. Rising levels of atmospheric CO_2 are a strong driver of climate-induced vegetation changes (Allen et al., 2014). Anthropogenic CO_2 emissions account for approximately 66% of the total anthropogenic greenhouse forcing (Forster et al., 2007) and are thus largely responsible for contemporary and future

30 global climate change Parry et al. (2007). Rising CO_2 is expected to alter distributions of plant species and ecosystems (Parry et al., 2007) both indirectly through its influence on global temperatures and precipitation patterns (Cao et al., 2010), two main drivers of vegetation dynamics, and directly via its physiological effects on plants (Nolan et al., 2018). It is therefore of vital importance to understand how ecosystems respond to simultaneous increases in atmospheric CO_2 and temperature, changes in precipitation regime, and altered ecosystem water balance in order to avoid critical ecosystem disruptions and the resulting

35 consequences for biodiversity and humankind.

Increases in temperatures, decreases in precipitation as well as changes in precipitation seasonality can cause loss of vegetation biomass. Elevated atmospheric CO_2 may influence vegetation due to the CO_2 fertilization effect (Curtis and Wang, 1998; Norby and Zak, 2011) that can influence photosynthesis, respiration, decomposition (Doherty et al., 2010), evapotranspiration (ET) and biomass accumulation (Frank et al., 2015). These CO_2 effects on plant growth and competition can alter community

40 structure, ecosystem productivity, climatic niches of ecosystems and biome boundaries (Nolan et al., 2018; Wingfield, 2013)). The physiology of C_3 plants leads to increased carbon fixation efficiency at elevated levels of atmospheric CO_2, improves their ability for carbon uptake, and thereby increases carbon sequestration (Leakey et al., 2009; Norby and Zak, 2011) as well as plant water use efficiency (Soh et al., 2019).

Long-term Free-Air Carbon dioxide Enrichment (FACE) experiments have demonstrated the productivity-enhancing effect

45 of elevated CO_2 (Norby and Zak, 2011). These effects are due to the fact that C_3 photosynthesis is not saturated at current atmospheric levels and thus C_3 plants benefit from increasing CO_2 (Ainsworth and Rogers, 2007). In contrast, C_4 plants are at their physiological optimum at current atmospheric CO_2. Increasing CO_2 concentration has been associated with woody cover increase in structurally open tropical biomes such as grasslands and savannas (Stevens et al., 2017). This widespread proliferation of woody plants in arid and semiarid ecosystems has been attributed to increased water use efficiency in C_3 plants

50 that facilitates woody sapling establishment and growth due to higher drought tolerance (Kgope et al., 2010; Stevens et al., 2017). Change in vegetation distribution and altered vegetation structure feed back on climate by altering fluxes of energy, moisture and CO_2 between land and atmosphere (Friedlingstein et al., 2006). Feedback mechanisms also involve vegetation-mediated changes in albedo, evapotranspiration, surface roughness and land-atmosphere fluxes (Field et al., 2007; Richardson et al., 2013).

55 Ecosystem-level ET is a key ecophysiological process in the soil-vegetation-atmosphere continuum (Feng et al., 2017). Annually, 64% of the total global land-based precipitation is returned to the atmosphere through ET (Zhang et al., 2016). Environmental change and concurrent vegetation changes alter ET and affect water availability (Mao et al., 2015), especially

in arid and semiarid regions. In these regions, ET affects surface and subsurface processes such as cloud development, land surface temperature, and groundwater recharge (Fisher et al., 2011).

60   South Asia is home to approx. 1.7 billion people and is one of the regions most vulnerable to climate change (Eckstein et al., 2018). It hosts four of the world's biodiversity hotspots (Myers et al., 2000) and harbors different biome types ranging from tropical in the south to temperate in the north at the fringe of the Himalayas. These hotspot are characterized by high levels of diversity and endemism, and they are threatened by climate change and anthropogenic pressure such as land-use (Deb et al., 2017). For instance, woody encroachment due to rising CO_2 threatens South Asian savannas (Kumar et al., 2020) and sifting

65   cultivation in north eastern part of South Asia threatens biodiversity (Bera et al., 2006).

Due to the absence of long-term field experiments such as FACE experiments, in the dominant biome types of the region, modeling studies are valuable tools to close existing knowledge gaps. Dynamic vegetation models (DGVMs, Prentice et al., 2007) are particularly well-suited to address questions that focus on vegetation response to changing environmental drivers, e.g., climate and CO_2. While most DGVM studies in South Asia focused on vulnerability of forests to climate change

70   (Chaturvedi et al., 2011; Ravindranath et al., 2006, 1997)they often overlooked the severely threatened savanna biome. They were further limited when using contemporary environmental conditions to pre-define bioclimatic limits of plant functional types (PFTs), and when using fixed eco-physiological parameters, for example to model carbon allocation. Moreover, many DGVMs do not account for life history, eco-evolutionary processes and trait variability among individual plants (Kumar and Scheiter, 2019). While some global-scale studies have investigated the potentially disruptive effect of increasing CO_2 on natural

75   vegetation, carbon sequestration and biome boundaries (e.g., Hickler et al.; Sato et al., 2007; Smith et al.), detailed modeling studies focusing explicitly on South Asia have not been conducted. The physiological effects of increased CO_2 and climate change on South Asian vegetation is uncertain and needs to be resolved narrowed in order to improve understanding of regional ecosystem functioning as well as implications for biodiversity conservation.

To address the knowledge gaps in existing studies, we used the aDGVM2 (adaptive dynamic global vegetation model version

80   2), an individual- and trait-based vegetation model that combines elements of traditional DGVMs (Prentice et al., 2007) with a new approach that allows community assembly resulting from environmental filtering applied to traits of modeled plant individuals (Langan et al., 2017; Scheiter et al., 2013). The aDGVM2 thus overcomes the shortcoming of using pre-defined and static PFTs. Originally, aDGVM2 had been tested for Amazonia Langan et al. (2017) and Africa (Gaillard et al.; Pfeiffer et al., 2019). In order to adapt it to South Asian ecosystems and to capture the diversity of South Asian ecosystems, we

85   included C_3 grasses, improved ecophysiological processes such as the leaf energy budget in order to estimate leaf temperature, implemented separate temperature sensitivities for C_3 and C_4 photosynthetic capacity (V_{cmax} and included snow in the water balance model.

In this study we used the updated version of aDGVM2 and addressed the following questions:

1. How do projected changes in climate and CO_2 following two Representative Concentration Pathways (RCP8.5 and

90   RCP4.5, Meinshausen et al., 2011) change the distribution, boundaries and climatic niches of biomes in South Asia?

2. How does the relationship between projected biomass, ET, temperature and precipitation change in response to CO_2 fertilization?

3. What is the sensitivity of predicted changes in relation to presence and absence of CO_2 fertilization?

Based on our results we analyzed climate-vegetation interactions to improve our understanding on how to manage and mitigate
95 impacts on biomes under climate change and increasing CO_2.

2   Methods

2.1   Description of the study region

Approx. 1.7 billion people populate South Asia, i.e., the Indian subcontinent, Afghanistan and Myanmar. South Asia incor-
porates a wide range of bio-climatic zones with distinctive biomes, ecosystem types, communities and species (Rodgers and
100 Panwar, 1988). Climatic conditions are controlled by interactions between the South Asian summer monsoon system and the
region's complex topography. The climatic envelope ranges from tropical arid and semi-arid regions in the west, to humid
tropical regions supporting rainforests in the northeast and temperate vegetation at the fringe of the Himalaya. Excluding the
Himalayan regions, South Asia has a mean annual temperature of approximately 24°C with very low spatial variability. Mean
annual precipitation (MAP) is 1190 mm, ranging from less than 500 mm in the warm desert zone in the west to more than 3500
105 mm in the northeast. The steep elevation gradients ranging from sea level to 8800 m result in a rich diversity of ecosystems that
can alternate in areas of a few hundred square-kilometers. Topography is recognized as a strong driver of ecological patterns,
for example those related to forest structure and composition, floristic diversity, and soil fertility (Gallardo-Cruz et al., 2009;
Jucker et al., 2018; Sinha et al., 2018). South Asia hosts four major global biodiversity hotspots, namely the Western Ghats, Hi-
malayas, Indo-Myanmar and Sri Lanka (www.conservation.org, Conservation International, 2013, Myers et al., 2000). These
110 hotspots include a wide diversity of ecosystems such as mixed wet evergreen, dry evergreen, deciduous, and montane forests.
Further vegetation types are alluvial grasslands and subtropical broadleaf forests along the foothills of the Himalayas, temper-
ate broadleaf forests in the mid hills, mixed conifer and conifer forests in the higher hills, savanna in the Deccan region and
southern part of Malaysia, and alpine meadows above the tree line (Conservation International, 2013).

2.2   Model Description

115 For this study we used aDGVM2, a DGVM that uses a dynamic trait approach. All details of the model are provided in Scheiter
et al. (2013), Langan et al. (2017) and Gaillard et al.. We summarize main features of aDGVM2 in the supplementary material.
To adapt the aDGVM2 to the requirements of the study region, we incorporated new sub-routines into the model. We improved
the representation of (a) the water balance by including snow, (b) the carboxylation rate, (c) leaf temperature, and (d) we
included C_3 grasses (previous model versions only simulate C_4 grasses).
120 (a) Water balance. In aDGVM2, the soil water module is based on the tipping-bucket concept. As the model was originally
developed with strong focus on tropical and subtropical forest and savanna regions, the original model version only considered

water input in form of rain (see Langan et al., 2017). In the updated model version, precipitation is assigned as snow when daily mean air temperature drops below 0°C. Snow accumulates on the soil surface or is added to the top of an existing snowpack. The snowpack persists as long as air temperature remains below 0°C. Once temperature rises above 0°C, water from snowmelt

125 is added to the soil water pool and becomes available to plants. This process may improve the water availability for plants at the beginning of spring, for example in the Himalayan region. Snowmelt (S_melt, mm/day) is calculated following (Choudhury et al., 1998) as

$$S_{melt} = 1.5 + K_m P_{precip}(T_a - T_{snow})S_{pack}, \tag{1}$$

where K_m is the coefficient of snowmelt (0.007 mm/day/ °C), Spack is the depth of the snowpack, T_a is daily mean air
130 temperature (°C), P_{precip} is precipitation (mm/day) and T_{snow} is the maximum temperature where precipitation falls as snow (0°C). We do not consider insulation effects of the snowpack in the model.

(b) Carboxylation rate.

In earlier versions of aDGVM2, leaf-level photosynthesis was calculated at population level, i.e., it was assumed that all plants of a simulated representative vegetation stand have the same leaf-level photosynthetic rate. Only C₃- and C₄-type photo-
135 synthesis were distinguished. We therefore implemented new routines to calculate photosynthesis at a daily time step for each individual plant. This version of aDGVM2 now incorporates an empirical relation between specific leaf area (A_{SLA}, mm²/mg) and leaf nitrogen content per unit area (N_a, g/m²) following Sakschewski et al. (2015),

$$N_a = 6.89 A_{SLA}^{-0.571}, \tag{2}$$

The standard maximum carboxylation rate of rubisco per leaf area (V_cmax,25, μmol/m²/s) was derived from the TRY database
140 Kattge and Knorr (2007) by Sakschewski et al. (2015) and is calculated as

$$V_{cmax,25} = 31.62 N_a^{0.501}, \tag{3}$$

where $V_{cmax,25}$ is V_{cmax} at 25°C.

In the model, A_SLA is linked to the matric potential at 50% loss of xylem conductance (P50, see Langan et al., 2017). The trade-off between A_SLA and V_cmax mediated by leaf traits (N_a) introduces variability in the spectrum of tree growth strategies in
145 aDGVM2. The effect of temperature on photosynthesis is well-described (Kirschbaum, 2004), and temperature may influence photosynthesis both directly, via temperature-dependency of enzyme-mediated metabolic rates of carboxylation and the Calvin cycle (Sharkey et al., 2007), and indirectly via its effect on transpiration and plant water uptake and transport (Urban et al., 2017). The maximum carboxylation rate (V_cmax) increases with temperature until it reaches an optimum, and decreases again at temperatures above the optimum (Kattge and Knorr, 2007) due to reductions in enzyme activity. Above 30°C the electron
150 transport chain is gradually inhibited, and at temperatures above 40°C the denaturation of Rubisco and associated proteins becomes relevant (Lloyd et al., 2008). The temperature dependency of the carboxylation rate (V_cmax) is expressed as

$$V_{cmax} = \frac{V_{cmax,25} 2^{0.1(T_{leaf}-25)}}{(1+e^{0.3(T_{low}-T_{leaf})})(1+e^{0.3(T_{leaf}-T_{upp})})}, \tag{4}$$

where T_{leaf} is the leaf temperature in °C (see next paragraph for calculation). The photosynthetic model of Collatz et al. (1992) and Collatz et al. (1992) assumes specific values of T_{upp} and T_{low} for C_3 and C_4 plants, respectively (Table S1 and Table S2). This temperature range allows plants to grow most efficiently in their plant-specific climatic niches.

(c) Leaf temperature. We calculate leaf temperature following the leaf-level energy budget concept (Gates, 1968). Leaf-level photosynthesis, activity of leaf enzymes and transpiration depend on leaf temperature (T_{leaf},°C), calculated as

$$T_{leaf} = T_{air} + (\frac{R_n - \lambda E r_{gb}}{\rho C_P}), \tag{5}$$

where T_{air} is air temperature (°C), R_n is net radiation absorbed by the leaf (MJ/m2/day), λ is latent heat of vaporization (MJ/kg), E is evapotranspiration (m/day), r_{gb} is the boundary layer resistance (m/s), ρ is the air density (kg/m³) and C_P is the specific heat of dry air (MJ/kg/°C). Leaf temperature is used to calculate the temperature dependence of V_{cmax} used in the photosynthesis model routines in equation (4). Absorbed net radiation (R_n), r_{gb} and E are model state variables calculated from climate input used in aDGVM2 (T_{air}, long-wave and short-wave radiation). Latent heat of vaporization (λ, ρ and C_P are assumed as constant parameters in this model version.

(d) C_3 grasses. C_3 grasses were not included in previous aDGVM2 versions (Gaillard et al.; Langan et al., 2017; Pfeiffer et al., 2019; Scheiter et al., 2013). We therefore implemented C_3 grasses, following the approach used for C_4 grasses in previous model versions but adjusted the photosynthetic pathway (see Appendix S2 in Langan et al., 2017).C_3 and C_4 grasses use a different leaf-level photosynthesis model (Farquhar et al., 1980) following the implementations of Collatz et al. (1991, 1992). The optimum temperature ranges for carboxylation for C_3 and C_4 grasses are also different (Table S1). Since C_3 grasses have higher cold tolerance than C_4 grasses (Liu and Osborne, 2008), we implemented frost intolerance for C_4 grasses but not for C_4 grasses. Frost is assumed to damage the tissue of C_4 grasses, and in aDGVM2 we kill 10% of the living leaf biomass of C_4 grasses per frost day independent of frost severity. A representation of C_3 grasses in aDGVM2 is necessary for this study to be able to simulate C_3-dominated biomes such as the C_3 grasslands in the north of South Asia (Quade et al., 1995).

2.3 Climate data

We used GFDL-ESM2M climate data for the period 1950 to 2099 from the Inter-Sectoral Impact Model Inter-comparison Project (ISIMIP2), as historical climate simulated by GFDL-ESM2M showed satisfactory performance over for South Asia (McSweeney and Jones, 2016). The general circulation model (GCM) output was bias-corrected in ISIMIP and downscaled to a spatial resolution of 0.5° × 0.5° (Warszawski et al., 2014). We used average, maximum and minimum air temperatures, precipitation, surface downwelling shortwave radiation and long-wave radiation, near-surface wind speed, and relative humidity at a daily temporal resolution. We used two representative concentration pathways, namely RCP4.5 and RCP8.5 (Meinshausen et al., 2011). These scenarios assume increases in radiative forcing of 4.5 and 8.5 Wm² by 2100 (Van Vuuren et al., 2011) and increases of atmospheric CO_2 concentrations to 560 ppm and 970 ppm by 2100, respectively (Van Vuuren et al., 2011).

2.4 Projected changes in temperature and precipitation

Mean annual precipitation (MAP) from GFDL-ESM2M shows decreases for South Asia under RCP4.5 and RCP8.5, except for
a small increase under RCP4.5 during the 2090s (2090-2099, Fig. S1). The Western Ghats and eastern Himalayan are projected
to become wetter under both RCP4.5 and RCP8.5, whereas the western part of the region is projected to become drier by the
end of the century under both RCPs (Fig. S2). By the end of the 21st century, mean annual temperature (MAT) of South Asia is
expected to increase between ca. 1°C and 3.5°C under RCP4.5 and between 1°C and 6°C under RCP8.5, relative to the average
temperature in the baseline period of 2000–2009 (Fig. S1 and Fig. S2). The western parts of the region and the Himalayan
mountains are projected to experience higher increases in temperature than the rest of the region (Fig. S2).

2.5 Soil and elevation data

Soil data was obtained from FAO (http://www.fao.org/soils-portal, Nachtergaele et al., 2009) and includes information on soil
properties and types. The soil properties include parameters required by aDGVM2: volumetric water-holding capacity, soil
hydraulic conductivity, soil bulk density, soil depth, soil texture, soil carbon content, soil wilting point and field capacity (for
details see Langan et al., 2017). A digital elevation model (DEM) at 90m spatial resolution was obtained from the Shuttle
Radar Topography Mission (SRTM, http://srtm.csi.cgiar.org, Jarvis et al., 2008). It was resampled to a spatial resolution of
$0.5° \times 0.5°$, to match the spatial resolution of climate data. Elevation values were used to estimate surface pressure. We did not
use slope and aspect in the model.

2.6 Model simulation protocol

Using the updated version of aDGVM2, we simulated four different scenarios for South Asia at $0.5° \times 0.5°$ spatial resolution.
We simulated potential natural vegetation until 2099 using daily climate data for RCP4.5 and RCP8.5. For both scenarios,
simulations were run with CO_2 increase in line with RCP4.5 (hereafter RCP4.5+eCO_2) and RCP8.5 (hereafter RCP8.5+eCO_2)
and with the same climate data but fixed CO_2 after 2005 at 375 ppm for RCP4.5 (hereafter RCP4.5+fCO_2) and RCP8.5
(hereafter RCP8.5+fCO_2). Fixing the CO_2 concentration after 2005 mimics a situation where CO_2 fertilization would not
occur and vegetation only responds to the climate signal. All simulations were conducted with natural fire as implemented in
aDGVM2.

To ensure that simulated vegetation had sufficient time to adapt to prevailing environmental conditions, we conducted sim-
ulations for 650 years, split into a 500 year spin-up phase and a 150 year transient phase. For the spin-up phase, we randomly
sampled years of the first 30 years of daily climate data (1950 to 1979). For the transient phase, we used the sequence of
daily climate data between 1950 and 2099. Trial simulations showed that a 500 year spin-up period is sufficient to ensure that
vegetation is in a dynamic equilibrium state with environmental drivers.

2.7 Model benchmarking and evaluation

For benchmarking of aDGVM2 simulation results, we used five different remote sensing products: aboveground biomass (Saatchi et al., 2011), tree height (Simard et al., 2011), tree cover (Friedl et al., 2010), MODIS evapotranspiration (Zhang et al., 2010) and natural vegetation type (Ramankutty et al., 2010). All remote sensing data sets were aggregated to a 0.5° × 0.5° spatial resolution, to match the spatial resolution of model simulations by calculating the mean of all values within each 0.5° grid cell, or using nearest neighbor aggregation in the case of vegetation type ("raster" package in R, Hijmans and van Etten, 2012). We first compared model results and observations assuming that the entire study region is covered by natural vegetation (Figs.1 and 2). Then we repeated the comparisons only for areas with predominantly natural cover, i.e., we masked out areas with more than 50% managed land (Figs. S3 and S4, land cover classes 7 'Cultivated and Managed Vegetation' and 9 'Urban and Built-up' in, Tuanmu and Jetz, 2014). We calculated Normalized Mean Squared Error (NMSE) and coefficient of determination (R^2 to quantify agreement between data and simulated variables.

2.8 Biome classification

The aDGVM2 simulates state variables such as biomass and canopy cover of individual plants in simulated vegetation stands (1 hectare). We used woody canopy area, abundance of shrubs and trees, and grass biomass to classify the simulated vegetation into biome types (Fig. S5). We used 10-year averages of state variables for the periods 2000-2009, 2050-2059 and 2090-2099 to represent the 2000s, 2050s and 2090s, respectively. Biome classification is often study-specific and to some degree subjective (Torello-Raventos et al., 2013). Here we classified areas with canopy cover below 5% as barren if grass biomass was below 100 kg/ha, and as grassland if grass biomass exceeded 100kg/ha. Grassland was classified as C_3 grassland or C_4 grassland based on predominance of respective biomass proportions. Simulated woody individuals were classified as trees if they had three or less stems and as shrubs if they had four or more stems. If tree canopy cover exceeded shrub canopy cover and was between 5% and 45%, then vegetation was classified as woodland if grass biomass was below 100kg/ha and as savanna if grass biomass was above 100kg/ha (Kumar, 2000). Savanna was further separated into C_4 savanna or C_3 savanna based on the dominant grass biomass. Areas with canopy cover greater than 45% were classified as forests if tree cover exceeded shrub cover, or shrubland if shrub cover exceeded tree cover, irrespective of grass biomass (Fig. S5). Forests were subdivided into evergreen and deciduous forest based on the dominance of canopy area of both tree phenology types. Biomes considered in this study were hence C_3 grassland, C_4 grassland, shrubland, woodland, deciduous forest, evergreen forest, C_3 savanna and C_4 savanna (Fig. S5).

Biomes differ in the amount of precipitation they receive and their temperatures. Whittaker plots describe the boundaries of observed biomes with respect to average temperature and precipitation. We used R-package ('plotbiomes', https://github.com/valentinitnelav/plotbiomes by Valentin Ștefan) to create Whittaker plot based on Ricklefs (2008) and (Whittaker, 1978)(Figs. 8 and S9). We overlaid the simulated biomes on Whittaker plots to look at climatic niches of biomes under current climate and shifts in climatic niches by the end of this century as a result of climate change and elevated CO_2 under both RCPs (see section 3.6).

2.9 Calculation of biome-level evapotranspiration

245 For analyzing evapotranspiration change we calculated the amount of water transpired per unit leaf biomass. Simulated ET and leaf biomass for woody plants, C_3 grass and C_4 grass were summed and scaled to the grid level, taking latitudinal variation of grid cell area into account. As leaf biomass influences transpiration we normalized ET to leaf biomass per grid cell. We then calculated the biome-level ET normalized to biomass as ratio of total annual ET to total leaf biomass for respective biomes:

$$E_{biome} = \frac{\sum_{i=1}^{G}(E_{grid,i} A_{grid,i})}{\sum_{i=1}^{G}(B_{grid,i} A_{grid,i})} \tag{6}$$

250 where 1, 2, ..., G represent the grid cells of the study area, E_{biome} is biome-level ET (mm/kg/year), $A_{grid,i}$ is the area of grid cell i (m^2, $E_{grid,i}$ is total ET of grid cell i (mm/year), $B_{grid,i}$ is leaf biomass of grid cell i (kg/m^2). We calculated the percentage change in E_{biome} for respective scenarios between the 2010s and 2050s, and between the 2010s and the 2090s.

3 Results

3.1 Model performance and contemporary vegetation patterns

255 The aDGVM2 captured contemporary large-scale patterns of biomass, canopy cover, tree height and evapotranspiration. Model results agreed well with remote sensing products used for benchmarking (Fig.1). R^2 was 0.61, 0.45, 0.6 and 0.71, and NMSE was 0.48, 0.78, 0.4 and 1.07 for biomass (Saatchi et al., 2011), tree height (Simard et al., 2011), tree cover (Friedl et al., 2010) and evapotranspiration (Zhang et al., 2010), respectively (Figs.1 and 2). Data-model agreement improved when masking out managed land (Tuanmu and Jetz, 2014). R^2 increased to 0.66, 0.71, 0.67 and 0.80, while NMSE increased to 0.43, 0.30, 0.61

260 and 1.03 for biomass, tree height, tree cover and evapotranspiration, respectively (Fig. S3 and S4). The model performed well in areas with higher fractional cover of natural vegetation, such as the Himalayas, Western Ghats and the northeast of the region, although the model overestimated biomass and canopy area in the Brahmaputra basin in the northeast of the study region (Fig.1, Kumar et al., 2020).

The model simulated evergreen forests along the Himalayan mountains, southern part of the Western Ghats and Sri Lanka,
265 whereas deciduous forest was simulated in the northern Western Ghats, central India and southern parts of Myanmar (Fig.3a). Savanna was simulated in southern, northern and western parts of India and some regions of central Myanmar. Shrublands were simulated in the arid regions of Pakistan, the western parts of India and Afghanistan. The aDGVM2 simulated woodland in the west of central India, and grassland in the drier regions (Fig.3a). A large proportion of simulated deciduous forest area is in good agreement with that in maps of potential natural vegetation (PNV, Figs.3b,c). However a large quantity of simulated
270 savanna area is misrepresented as deciduous forest in the map of PNV (Fig.3b, Kumar et al., 2020).

3.2 Projected changes in biome distribution pattern

The aDGVM2 projected changes in canopy cover and above ground biomass in response to climate change and CO_2, and hence, changes in biome type, predominantly from savanna and grassland to deciduous forest. Simulations showed an increase

in the area covered by evergreen and deciduous forests under elevated CO_2 (eCO_2) under both RCP4.5 and RCP8.5, in con-
275   trast to simulations where CO_2 was fixed after 2005 (fCO_2, (Table.1). Under RCP4.5+eCO_2, evergreen and deciduous forest
cover increased by 3.1% and 21.2% until the 2050s, and 38.0% and 59.1% until the 2090s, respectively. Under RCP8.5+eCO_2,
evergreen and deciduous forest increased by 24.8% and 45.4% until the 2050s, and 46.5% and 60.2% until the 2090s, respec-
tively. The model simulated a small increase in forest area for RCP4.5+fCO_2, where the area increased by 7.9% and 14.4% for
evergreen and deciduous forest until the 2090s, respectively. Evergreen forests were mainly distributed along the Himalayas,
280   Western Ghats and eastern parts of the study region under current conditions (2000s, (Fig.4a), but expanded into the south of
peninsular India in future periods (2050s and 2090s) under RCP4.5+eCO_2. Deciduous forest cover also increased in future
periods in central India and along the Himalayas (Figs.4 and S6).

The extent of C_4 savanna showed a significant decrease under scenarios with eCO_2, although in RCP4.5+eCO_2, it showed
a temporary increase by 12.1% between the 2010s and the 2050s (Table. 1, Fig.4). Simulated C_4 savanna area decreased by
285   14.1% until the 2090s under RCP4.5+eCO_2. Under RCP8.5+eCO_2 the model projected a decrease in C_4 savanna area of 21.6%
and 32.2% until the 2050s and the 2090s, respectively. The area covered by C_4 savanna increased under both RCPs with fCO_2
(Table.1). C_4 savannas were mainly located in the northern plain and peninsular India in the baseline period. However, these
areas were replaced by deciduous forests in the northern plain and central India, and by evergreen forests in peninsular India
and in the southeast of the region by the 2090s under eCO_2 scenarios (Figs.4a and S6a). The model simulated an area decrease
290   for woodland, shrubland, grassland and C_3 savanna by the 2090s under all scenarios (Table. 1, Fig. 4). Simulations showed an
increase in barren areas in the western part of the region under all scenarios (Figs. 4 and S6, Table. 1).

3.3   Projected changes in biomass at biome level

The aDGVM2 predicted an increase in mean biomass for evergreen and deciduous forest in the eCO_2 scenarios for both RCPs
(Table. 2). Under RCP4.5+eCO_2, mean above ground biomass in evergreen and deciduous forest increased by 8.1% and 14.4%
295   by the 2050s and 3.8% and 15.7% by the 2090s, relative to the baseline period. The increase is even higher under RCP8.5+eCO_2
(Table. 2). The mean biomass of woodland decreased under both RCPs except for the 2050s with eCO_2 scenarios. The mean
biomass of grassland increased under RCP4.5, although it decreased for C_4 grassland under RCP8.5 for both fCO_2 and eCO_2
scenarios. Shrublands in the western part of the study region showed an increase in mean biomass under eCO_2 scenarios except
for the 2050s under both RCPs, and a decrease under fCO_2 for both RCPs (Table. 2). Our results showed that under RCP4.5
300   and RCP8.5 biomass decreased in the areas along the Himalayas, as well as in the central, north-eastern and western parts of
the study region by the end of the century. Modeled biomass decrease is higher under RCP8.5 in these regions (Figs. 5 and S7).
Biomass in the central and south-eastern part of the region is projected to increase under both RCPs with eCO_2 until the 2050s
and 2090s, and to decrease in southern India and in parts of western South Asia (Figs. 5 and S7). We found increased biomass
in Afghanistan, western Pakistan, Nepal and southern part of Myanmar, and decreased biomass in the western arid part of
305   the study region under both RCPs for both eCO_2 and fCO_2 (Fig.7), though the magnitude of change is considerably different
(Figs.5 and S7). There were few small areas in the western part of the study region where the model predicted increased

biomass only under fCO_2 for both RCPs (Figs.7). We found increased biomass over large part of the study region under eCO_2 for both RCPs shows areas (Figs.7) where CO_2 fertilization compensates climate change induced biomass die-back.

3.4   Projected changes in evapotranspiration at biome level

310   The response of simulated E_{biome} varies in different biomes under both RCP4.5 and RCP8.5 (Table. 3). Under the RCP4.5+fCO_2 scenario the model predicted a decrease in ET in all biomes except for deciduous forest and shrubland where it increased by 1% and 2.1% until the 2050s, and by 0.3% and 11.9% by the 2090s, respectively. Simulated E_{biome} under RCP8.5+fCO_2 for deciduous forest and shrubland increased by 4.2% and 5.2% until the 2050s, and by 5.2% and 16.4% until the 2090s, respectively. The model also predicted increased Ebiome for C_4 grassland, evergreen forest and C_4 savanna until the 2090s

315   under RCP8.5+fCO_2 (Table.3). Comparisons of the RCP4.5+fCO_2 and RCP8.5+fCO_2 scenarios indicated that the former had a higher E_{biome} than the latter scenario across all biomes because precipitation decrease is higher in the RCP8.5 scenario than in the RCP4.5 scenario. Under both RCPs with eCO_2, the model predicted a decrease in E_{biome} across all biomes, except a marginal increased E_{biome} for shrubland under RCP4.5 and deciduous forest under RCP8.5 until the 2050s and the 2090s (Table. 3). In general, RCP scenarios with eCO_2 predicted reduced E_{biome} across most of the biomes compared to simulations

320   with fCO_2.

3.5   Response of mean ET and mean above ground biomass to climate change

The model predicted a larger increase in absolute annual mean ET (mm/year) under eCO_2 than fCO_2 for both RCP scenarios due to the corresponding increase in biomass (Figs. 5 and S7). We compared the spatially averaged annual values of simulated absolute ET with MAP over the period from 1951 to 2099 and found a statically significant relation (p-value <0.005). We

325   found that absolute ET is positively correlated with MAP under all four scenarios (Figs.6a and S8a), but weakly correlated with MAT (Figs. 6b and S8b). For a given MAP, the spatially averaged annual value of above ground biomass (AGBM) was lower in scenarios with fCO_2 than scenarios with eCO_2 under both RCPs (Figs. 6c and S8c). Spatially averaged annual value of AGBM decreased beyond a MAT of 23.5°C for both RCPs with fCO_2, whereas it increased beyond 23.5°C under both RCP scenarios with eCO_2 (Figs.6d and S8d).

330   ## 3.6   Impact of climate change on climatic niches of biomes

The climate niches of simulated biomes broadly overlapped with biome niches in the Whittaker scheme (Figs. 8 and S9, Ricklefs, 2008; based on Whittaker, 1975). Under RCP4.5+eCO_2 and RCP8.5+eCO_2, the aDGVM2 simulated shifts of climatic niches of biomes. Evergreen and deciduous forest biomes were predicted to invade the niche space of savannas under eCO_2 scenarios (Figs.5 and S9). Savannas in turn were predicted to expand their climatic niche to MAT > 30°C by 2099, a climatic

335   space that was essentially not occupied by current biomes. Under RCP8.5+eCO_2, forests completely occupied the climate space currently occupied by savanna (Fig. S9).

In both scenarios with fCO$_2$, savanna occupied the climate with MAT >25°C and MAP between 500mm and 1500mm and did not show major woody encroachment. The model predicted that savanna expansion in climate space was higher under RCP8.5+fCO$_2$ than under RCP4.5+fCO$_2$ (Figs.8 and S9). Other biomes also experienced shifts in their climate space (Fig. 8). Grasslands and shrublands occupied the region with low MAP (<500mm), however the results showed that woodland also occupied low MAP (<800mm) regions, which corresponds to the western arid and semi-arid region of the study region under scenario with eCO$_2$ (Fig. 8).

4 Discussion

4.1 Impact of climate change and elevated CO$_2$ on biomes and biomass

Our simulations for RCP4.5+eCO$_2$ and RCP8.5+eCO$_2$ showed a strong positive impact on vegetation growth, i.e., increases of biomass, canopy cover and canopy height. Mean biomass in most biomes was projected to increase, but the magnitude of increase differed considerably between different scenarios (Table.2). Projected change in canopy cover resulted in biome transitions. Under future conditions, the spatial distribution, extent and biomass of evergreen forests mostly remained at the current state, and evergreen forests were more resistant to climate change than deciduous forests. Expansion of deciduous forest into open biomes due to increasing woody cover resulted in significant loss of savanna area in the Deccan region under both RCPs with eCO$_2$ by the end of the century. Transition from deciduous forests to evergreen forest was simulated for the mountain regions of South Asia.

The increasing woody biomass and canopy cover, i.e., woody encroachment, agree with the reported greening trend in South Asia during the last three decades (Wang et al., 2017). Increasing CO$_2$ has been identified as the most likely driver of increasing biomass in many ecosystems, in studies based on both field observation e.g., FACE experiments, and satellite data (Brienen et al., 2015; Fischlin et al., 2007; Piao et al., 2006; Schimel et al., 2015). Elevated CO$_2$ affects plants by increasing their photosynthetic rate, growth rate and water use efficiency, leading to an increase in biomass (Leakey et al., 2009; Norby and Zak, 2011). Increased photosynthetic rates under elevated CO$_2$ are due to an increase in the rate of rubisco carboxylation for C$_3$ plants, with a concurrent decrease of photorespiratory losses of carbon (Long et al., 2004). Due to the improved carboxylation efficiency, C$_3$ plants can respond by reducing stomatal conductance, thereby reducing transpirational losses, improving leaf water status, water use efficiency, and favoring leaf area growth (Long et al., 2004; Norby and Zak, 2011). However, it is still unclear how these responses scale to the ecosystem level (Hickler et al., 2015), and how nutrient limitation from the soil may influence ecosystem responses to eCO$_2$. Körner (2015) argued that carbon from atmosphere can only be converted into biomass if other factors such as nutrients, temperature and water are not limiting. In the long run, whether ecosystems act as carbon source or sink can be estimated using models that consider all factors that are relevant in the carbon cycle (Fatichi et al., 2014; Körner, 2015). According to our simulations we can conclude that natural vegetation of South Asia likely will remain a carbon sink in the future.

4.2 Impact of climate change and fixed CO_2 on biomes and biomass

Under both fCO_2 scenarios, the spatial distribution of savanna areas remained in its contemporary state. Central India and the
370 Deccan Plateau showed a transition of deciduous forest to savanna, because forest canopy opened up due to tree mortality
caused by increasing temperature and reduced MAP. This indicates that plants experience temperature and drought stress un-
der fixed CO_2 concentration. These stresses were compensated by CO_2 fertilization in eCO_2 scenarios where the aDGVM2
simulated increased biomass and woody encroachment in areas affected by climate-induced die-back in fCO_2 simulations.
This aDGVM2 behavior agrees with, Lapola et al. (2009) who modeled biome shifts from forest to savanna in absence of
375 CO_2 fertilization for the Amazon region. Changes in precipitation regimes are likely to have a strong influence particularly in
arid and semi-arid regions, such as grasslands (Verstraete et al., 2009). The complex interactions of inter-annual precipitation
variability and precipitation seasonality can result in rapid ecosystem transitions (e.g., between alternative stable states with
high and low vegetation biomass; Holmgren and Scheffer, 2001). The decrease in simulated AGBM after MAT increases be-
yond 23.5°C under fCO_2 scenarios can be explained by the longer exposure of vegetation to temperatures beyond the optimum
380 temperature range of C_3 photosynthesis during the main growing season. This effect was further enhanced by decreasing MAP
and the absence of CO_2 fertilization. This implies that the increase in MAT above 23.5°C together with weak CO_2 fertilization
would have negative consequences for carbon sequestration. It also implies that we need a better understanding of impacts
of heat stress on vegetation and how it interacts with drought and CO_2 fertilization. It is also unclear to what degree thermal
acclimation may counteract some of the negative effects on plant growth caused by higher temperatures (Lombardozzi et al.,
385 2015).

4.3 Impact of climate change and CO_2 change on climatic niches of biomes

Elevated CO_2 has a major impact on the climatic niche space of biomes, especially the climatic envelope of savannas. Our
simulations indicated that forest invaded the niche space currently occupied by savanna by the end of the century. The expansion
of forests to drier areas corresponds to a widening of their climate niche space under eCO_2. This expansion is corroborated by
390 the fact that in absence of CO_2 fertilization the climatic niche of biomes is stable, i.e., biomes occupy the same niche under
current and future conditions. These findings imply that the bioclimatic boundaries used to define biome niche space are not
static, but are specific for given CO_2 levels. Therefore, the thresholds of the Whittaker's biomes need to be redefined for a
high-CO_2 world such that they encompass the altered climatic envelopes of biomes under elevated CO_2 in future (Fig. 5). The
shift in niche space can be attributed to the shift in plant communities caused by the combined effect of climate change and
395 elevated CO_2, which increases plant water efficiency allowing them to grow in harsh condition. These shift can also lead to
change the characteristics of biomes by altering community structure and ecosystem functions (Chapin et al., 1997).

4.4 Effect of CO_2 on ET and its interaction with climate change

Climate change has direct effects on hydrological processes (Liu et al., 2008). ET and water deficit influence plant productivity
and distribution (Stephenson, 1998). Higher biomass resulted in increased absolute amounts of ET for eCO_2 scenarios in some

400 parts of the study region under both RCPs by the end 21st century (Figs. 5 and S7). This change can be attributed to the fact
that plants accumulated higher biomass while reducing stomatal conductance due improved water use efficiency under eCO_2
scenarios and resulted in reduced ET per unit leaf biomass (Warren et al., 2011). Our results showed that the strength of the
CO_2 fertilization effect is relevant when attempting to determine E_{biome} at biome level during the 21st century. Biome-specific
ET decrease was less pronounced under RCP4.5 due to a lower concentration of atmospheric CO_2 compared to RCP8.5. Our
405 simulated decrease in ET in response to climate change and increasing CO_2 concentration agrees with Kergoat et al. (2002) who
have reported decreased ET under elevated CO_2 concentration in a chamber experiment. However, reduced ET under eCO_2
can reduce regional-scale atmospheric humidity and thereby enhance the vapor pressure deficit (VPD), a driving force for
water loss, between leaves and the atmosphere, which may partially counteract CO_2-induced reduction of ET due to decreased
stomatal conductance. Projected increases in air temperature can also enhance atmospheric water storage capacity and VPD,
410 and thereby evapotranspiration may increase (Warren et al., 2011). As future climate projections vary spatially and temporally,
there was high model uncertainty on how ET will respond to changes in precipitation and temperature.

4.5 Implication of woody encroachment for water resources

Water is a limiting factor for vegetation in arid and semi-arid regions. Improved WUE of C_3-plants under eCO_2 boost produc-
tivity and therefore facilitated woody encroachment. However, increased woody cover can negatively affect water resources.
415 Acharya et al. (2018) showed that increased woody cover hinders the downward movement of water in the soil profile as result
of increased rooting depth and density in more densely-packed woody vegetation. Increased water inception through roots in
the soil can have negative effects for ground water recharge. It is therefore necessary to control the abundance of woody plants
in semi-arid regions to control streamflow and enhance groundwater recharge (Bednarz et al., 2001).

4.6 Implication of the projected change for conservation

420 Changes in biome types imply changes in biodiversity, ecosystem function and productivity. Each biome is characterized
by a range of distinctive ecological processes and functions. The distribution pattern of plants in the mountains is largely
regulated by the altitude and climatic factor (Saikia et al., 2017). These fragile ecosystems such as forests, in the mountains
have high species richness and needed to be protected from the ever-increasing anthropogenic pressure and climate change. In
the other hand, open biomes such as grassland and savanna support high biodiversity (Parr et al., 2014). Pronounced increases
425 in tree density in grasslands and savannas will alter vegetation structure and reduce grassland biodiversity. Such changes
will negatively affect savanna-specific ecosystem services such as grazing potential, tourism and wildlife habitat availability
(Parr et al., 2012). The threat posed to the biodiversity of Asian savannas by climate change is aggravated by inadequate
management policies that misinterpret them as degraded forest (Ratnam et al., 2016). In this context, management policies
aim to afforest open biomes, although paleo-ecological evidence indicates that these open biomes are not degraded forest but
430 ancient ecosystems (Kumar et al., 2020; Ratnam et al., 2016).

In South Asia, biodiversity hotspots have a very unique topography, where climate varies strongly over short distances. As
global biodiversity hotspots, mountain forest ecosystems in the Western Ghats, the Himalayas and northeastern part of the

study area (Indo-Myanmar) are particularly vulnerable to climate change (Myers et al., 2000) and need targeted management action to mitigate adverse effects. Conservation of these hotspots requires consideration of many different attributes of plant

435 communities, ecosystems, landscapes, and plant diversity, how they will change, and how their ecosystem services are valued.

Conservation methods and policies that can accommodate minimal losses of ecosystem services and provide robust strategies for mitigating climate change impacts should be developed and implemented. In this context, DGVMs facilitate the exploration of vegetation-climate interactions by providing detailed results for different management and climate scenarios. Such an exploration of different possible scenarios is necessary to develop optimized mitigation and conservation strategies for protected

440 areas in biodiversity hotspots. The value of DGVM modelling results lies in their potential to provide insights into multiple future trajectories. Based on the most likely trajectories, the results can be used to tailor best-practice strategies for decision makers that need to manage conservation areas or protected areas Boulangeat et al. (2012).

4.7 Limitations of this modelling study

Our simulation results are constrained by the model formulation and the assumptions underlying aDGVM2. Disagreement

445 between model results and data used for benchmarking can be attributed to the fact that the aDGVM2 simulates potential natural vegetation whereas remote sensing products integrate land use. This implies that enhancing the model to simulate observed land cover patterns would require additional information on anthropogenic impacts. Anthropogenic activities such as deforestation, habitat conversion and urbanization can modify the interactions between climate, plant communities and biomes (Hansen et al., 2001).

450 In addition data-model disagreement can be explained by uncertainties in aDGVM2 and processes currently not considered. For instance, the aDGVM2 uses carbon allocation parameters that are not easily measurable in the field, which is limits the evaluation of simulated mechanisms. The model currently lacks a representation of carbon that plants actively invest into nutrient acquisition (e.g. mycorrhiza) or to build defenses against predation and pathogens (Zemunik et al., 2015) and there is insufficient ecophysiological data from the region, required for parameterization of trait ranges used to simulate plant

455 communities (Kumar and Scheiter, 2019). The complexity of the interactions between global change and biomes as well as biodiversity is difficult to model in absence of such data. Further, the strength of CO_2 fertilization modelled in aDGVM2 may be overestimated, given that the model does not include nutrient limitation (Körner et al., 2005; Terrer et al., 2018). Despite these caveats, we are nonetheless confident to capture general patterns of future global change and its consequences for biodiversity in South Asia.

460 5 Conclusions

We investigated the impact of eCO_2 and climate change on South Asian vegetation with the aDGVM2. The model reproduced the contemporary distribution of biomes, biomass, ET and tree height. In comparison to fCO_2 simulations, we found that climate change and CO_2 fertilization in combination are substantial drivers of biome change, and that elevated CO_2 concentrations also altered the climatic envelope of biomes in addition to causing increases in biomass, tree height and canopy cover.
465 Continued biomass increase indicates that South Asia's natural vegetation will likely remain a carbon sink in the 21st century. Our results also imply woody encroachment posing threat to open biomes and causing transition of savanna biomes to deciduous forest in the future which are particularly critical aspect in the context of biodiversity conservation. Thresholds that define bioclimatic envelopes of biomes are not static, but are specific for given CO_2 concentrations which imply that these thresholds need to be adjusted to account for changed climatic niches caused by eCO_2 in the future. We also found that simulated decrease

470 in biomass-specific ET is more pronounced in scenarios with eCO_2 than in scenarios with fCO_2 which indicates that water use efficiency will likely increase due to CO_2 fertilization.

The biome transitions simulated under eCO_2 and changing climate indicate the need to adjust ecosystem management, mitigation strategies, and conservation policies for protected areas to allow targeted long-term management. To understand the significance of ecological responses to climate change, it is essential to improve and expand biological monitoring activities

475 (Loreau et al., 2001). To achieve this, most vulnerable biomes identified by modeling results such as the ones we present in this study could be proposed as high-priority targets for programs that monitor vegetation-climate interactions, productivity and biodiversity Proença et al. (2017).

Code availability. The aDGVM2 code as well as scripts to conduct the model experiments and analyze the results are available upon request. Please contact any of the authors.

480 *Author contributions.* DK and SS conceived the study, DK included changes to aDGVM2 for the study region, conducted model simulations, analyzed results, created figures and lead the writing. All authors contributed to the development of aDGVM2 and comments to the text.

Competing interests. The authors declare that they have no conflict of interest.

Disclaimer. Key words: aDGVM2, climate change, CO2-fertilization, biome shift, woody encroachment, evapotranspiration, biodiversity conservation, South Asia

485 *Financial support.* SS and DK thank the Deutsche Forschungsgemeinschaft (DFG) for funding (Emmy Noether grant SCHE 1719/2-1). MP acknowledges funding by the German Federal Ministry of Education and Research (BMBF, SPACES2 initiative, 'SALLnet' project, grant 01LL1802B).

.

References

490   Acharya, B. S., Kharel, G., Zou, C. B., Wilcox, B. P., and Halihan, T.: Woody plant encroachment impacts on groundwater recharge: A review, Water, 10, 1466, https://doi.org/10.3390/w10101466, 2018.

Ainsworth, E. A. and Rogers, A.: The response of photosynthesis and stomatal conductance to rising CO_2: mechanisms and environmental interactions, Plant, cell & environment, 30, 258–270, https://doi.org/10.1111/j.1365-3040.2007.01641.x, 2007.

Allen, M. R., Barros, V. R., Broome, J., Cramer, W., Christ, R., Church, J. A., Clarke, L., Dahe, Q., Dasgupta, P., and Dubash, N. K.: IPCC
495   fifth assessment synthesis report-climate change 2014 synthesis report, 2014.

Bednarz, S. T., Dybala, T., Muttiah, R. S., Rosenthal, W., and Dugas, W. A.: Brush/water yield feasibility studies, Blackland Research Center, Temple, Texas, USA, 2001.

Bera, S. K., Basumatary, S. K., Agarwal, A., and Ahmed, M.: Conversion of forest land in Garo Hills, Meghalaya for construction of roads: A threat to the environment and biodiversity, Current Science, pp. 281–284, publisher: JSTOR, 2006.

500   Boulangeat, I., Philippe, P., Abdulhak, S., Douzet, R., Garraud, L., Lavergne, S., Lavorel, S., Van Es, J., Vittoz, P., and Thuiller, W.: Improving plant functional groups for dynamic models of biodiversity: at the crossroads between functional and community ecology, Global change biology, 18, 3464–3475, https://doi.org/10.1111/j.1365-2486.2012.02783.x, 2012.

Brienen, R. J., Phillips, O. L., Feldpausch, T. R., Gloor, E., Baker, T. R., Lloyd, J., Lopez-Gonzalez, G., Monteagudo-Mendoza, A., Malhi, Y., and Lewis, S. L.: Long-term decline of the Amazon carbon sink, Nature, 519, 344–348, publisher: Nature Publishing Group, 2015.

505   Brodie, J. F., Aslan, C. E., Rogers, H. S., Redford, K. H., Maron, J. L., Bronstein, J. L., and Groves, C. R.: Secondary extinctions of biodiversity, Trends in Ecology & Evolution, 29, 664–672, https://doi.org/10.1016/j.tree.2014.09.012, 2014.

Cao, L., Bala, G., Caldeira, K., Nemani, R., and Ban-Weiss, G.: Importance of carbon dioxide physiological forcing to future climate change, Proceedings of the National Academy of Sciences, 107, 9513–9518, https://doi.org/10.1073/pnas.0913000107, 2010.

Chapin, F. S., Walker, B. H., Hobbs, R. J., Hooper, D. U., Lawton, J. H., Sala, O. E., and Tilman, D.: Biotic control over the functioning of
510   ecosystems, Science, 277, 500–504, https://doi.org/10.1126/science.277.5325.500, 1997.

Chaturvedi, R. K., Gopalakrishnan, R., Jayaraman, M., Bala, G., Joshi, N. V., Sukumar, R., and Ravindranath, N. H.: Impact of climate change on Indian forests: a dynamic vegetation modeling approach, Mitigation and Adaptation Strategies for Global Change, 16, 119–142, 2011.

Chen, I.-C., Hill, J. K., Ohlemüller, R., Roy, D. B., and Thomas, C. D.: Rapid range shifts of species associated with high levels of climate warming, Science, 333, 1024–1026, https://doi.org/10.1126/science.1206432, 2011.

515   Choudhury, B. J., DiGirolamo, N. E., Susskind, J., Darnell, W. L., Gupta, S. K., and Asrar, G.: A biophysical process-based estimate of global land surface evaporation using satellite and ancillary data II. Regional and global patterns of seasonal and annual variations, Journal of Hydrology, 205, 186–204, https://doi.org/10.1016/s0022-1694(97)00149-2, 1998.

Collatz, G. J., Ball, J. T., Grivet, C., and Berry, J. A.: Physiological and environmental regulation of stomatal conductance, photosynthesis and transpiration: a model that includes a laminar boundary layer, Agricultural and Forest meteorology, 54, 107–136,
520   https://doi.org/10.1016/0168-1923(91)90002-8, 1991.

Collatz, G. J., Ribas-Carbo, M., and Berry, J. A.: Coupled photosynthesis-stomatal conductance model for leaves of C4 plants, Functional Plant Biology, 19, 519–538, https://doi.org/10.1071/pp9920519, 1992.

Curtis, P. S. and Wang, X.: A meta-analysis of elevated CO_2 effects on woody plant mass, form, and physiology, Oecologia, 113, 299–313, https://doi.org/10.1007/s004420050381, 1998.

525   Deb, J., Phinn, S. R., Butt, N., and McAlpine, C. A.: Summary of climate change impacts on tree species distribution, phenology, forest structure and composition for each of the 85 studies reviewed, https://doi.org/10.14264/uql.2017.814, 2017.

Doherty, R. M., Sitch, S., Smith, B., Lewis, S. L., and Thornton, P. K.: Implications of future climate and atmospheric CO_2 content for regional biogeochemistry, biogeography and ecosystem services across East Africa, Global Change Biology, 16, 617–640, https://doi.org/10.1111/j.1365-2486.2009.01997.x, 2010.

530   Eckstein, D., Hutfils, M., and Winges, M.: Global climate risk index 2019: Who suffers most from extreme weather events? Weather-related loss events in 2017 and 1998 to 2017. Germanwatch, Bonn, Germany, 2018.

Farquhar, G. D., von Caemmerer, S. v., and Berry, J. A.: A biochemical model of photosynthetic CO_2 assimilation in leaves of C_3 species, Planta, 149, 78–90, https://doi.org/10.1007/bf00386231, 1980.

Fatichi, S., Leuzinger, S., and Körner, C.: Moving beyond photosynthesis: from carbon source to sink-driven vegetation modeling, New

535   Phytologist, 201, 1086–1095, https://doi.org/10.1111/nph.12614, 2014.

Feng, H., Zou, B., and Luo, J.: Coverage-dependent amplifiers of vegetation change on global water cycle dynamics, Journal of hydrology, 550, 220–229, https://doi.org/10.1016/j.jhydrol.2017.04.056, 2017.

Field, C. B., Lobell, D. B., Peters, H. A., and Chiariello, N. R.: Feedbacks of terrestrial ecosystems to climate change, Annu. Rev. Environ. Resour., 32, 1–29, https://doi.org/10.1146/annurev.energy.32.053006.141119, publisher: Annual Reviews, 2007.

540   Fischlin, A., Midgley, G. F., Price, J. T., Leemans, R., Gopal, B., Turley, C. M., Rounsevell, M. D. A., Dube, P., Tarazona, J., and Velichko, A.: Impacts adaptation and vulnerability. Contribution of Working Group II to the Fourth Assessment Report of the Intergovernmental Panel on Climate Change, M.L. Parry, O.F. Canziani, J.P. Palutikof, P.J. van der Linden and C.E. Hanson, Eds., Cambridge University Press, Cambridge, UK, 391-431, Assessment Report of the Intergovernmental Panel on Climate Change, 4, 211–272, 2007.

Fisher, J. B., Whittaker, R. J., and Malhi, Y.: ET come home: potential evapotranspiration in geographical ecology, Global Ecology and

545   Biogeography, 20, 1–18, 2011.

Forster, P., Ramaswamy, V., Artaxo, P., Berntsen, T., Betts, R., Fahey, D. W., Haywood, J., Lean, J., Lowe, D. C., and Myhre, G.: Changes in atmospheric constituents and in radiative forcing. Chapter 2, in: Climate Change 2007. The Physical Science Basis, 2007.

Frank, D., Reichstein, M., Bahn, M., Thonicke, K., Frank, D., Mahecha, M. D., Smith, P., Van der Velde, M., Vicca, S., and Babst, F.: Effects of climate extremes on the terrestrial carbon cycle: concepts, processes and potential future impacts, Global Change Biology, 21,

550   2861–2880, https://doi.org/10.1111/gcb.12916, 2015.

Friedl, M. A., Sulla-Menashe, D., Tan, B., Schneider, A., Ramankutty, N., Sibley, A., and Huang, X.: MODIS Collection 5 global land cover: Algorithm refinements and characterization of new datasets, Remote sensing of Environment, 114, 168–182, https://doi.org/10.1016/j.rse.2009.08.016, 2010.

Friedlingstein, P., Cox, P., Betts, R., Bopp, L., von Bloh, W., Brovkin, V., Cadule, P., Doney, S., Eby, M., and Fung, I.: Climate–carbon cycle

555   feedback analysis: results from the C4MIP model intercomparison, Journal of climate, 19, 3337–3353, https://doi.org/10.1175/jcli3800.1, 2006.

Gaillard, C., Langan, L., Pfeiffer, M., Kumar, D., Martens, C., Higgins, S. I., and Scheiter, S.: African shrub distribution emerges via height—Sapwood conductivity trade-off., https://doi.org/10.1111/jbi.13447.

Gallardo-Cruz, J. A., Pérez-García, E. A., and Meave, J. A.: β-Diversity and vegetation structure as influenced by slope aspect and altitude

560   in a seasonally dry tropical landscape, Landscape Ecology, 24, 473–482, https://doi.org/10.1007/s10980-009-9332-1, 2009.

Gates, D. M.: Transpiration and leaf temperature, Annual Review of Plant Physiology, 19, 211–238, https://doi.org/10.1146/annurev.pp.19.060168.001235, 1968.

Hansen, A. J., Neilson, R. P., Dale, V. H., Flather, C. H., Iverson, L. R., Currie, D. J., Shafer, S., Cook, R., and Bartlein, P. J.: Global change in forests: responses of species, communities, and biomes: interactions between climate change and land use are projected to cause large shifts in biodiversity, BioScience, 51, 765–779, 2001.

Herring, S. C., Christidis, N., Hoell, A., Kossin, J. P., Schreck III, C. J., and Stott, P. A.: Explaining extreme events of 2016 from a climate perspective, Bulletin of the American Meteorological Society, 99, S1–S157, https://doi.org/10.1175/bams-explainingextremeevents2016.1, 2018.

Hickler, T., Prentice, I. C., Smith, B., Sykes, M. T., and Zaehle, S.: Implementing plant hydraulic architecture within the LPJ Dynamic Global Vegetation Model, pp. 567–577, https://doi.org/10.1111/j.1466-8238.2006.00254.x.

Hickler, T., Rammig, A., and Werner, C.: Modelling CO 2 impacts on forest productivity, Current Forestry Reports, 1, 69–80, https://doi.org/10.1007/s40725-015-0014-8, 2015.

Hijmans, R. J. and van Etten, J.: raster: Geographic analysis and modeling with raster data. R package version 2.0–12, 2012.

Holmgren, M. and Scheffer, M.: El Niño as a window of opportunity for the restoration of degraded arid ecosystems, Ecosystems, 4, 151–159, https://doi.org/10.1007/s100210000065, 2001.

Jarvis, A., Reuter, H. I., Nelson, A., and Guevara, E.: Hole-filled SRTM for the globe Version 4, available from the CGIAR-CSI SRTM 90m Database, 2008.

Jucker, T., Bongalov, B., Burslem, D. F., Nilus, R., Dalponte, M., Lewis, S. L., Phillips, O. L., Qie, L., and Coomes, D. A.: Topography shapes the structure, composition and function of tropical forest landscapes, Ecology letters, 21, 989–1000, https://doi.org/10.1111/ele.12964, 2018.

Kattge, J. and Knorr, W.: Temperature acclimation in a biochemical model of photosynthesis: a reanalysis of data from 36 species, Plant, cell & environment, 30, 1176–1190, https://doi.org/10.1111/j.1365-3040.2007.01690.x, 2007.

Kergoat, L., Lafont, S., Douville, H., Berthelot, B., Dedieu, G., Planton, S., and Royer, J.-F.: Impact of doubled CO2 on global-scale leaf area index and evapotranspiration: Conflicting stomatal conductance and LAI responses, Journal of Geophysical Research: Atmospheres, 107, ACL–30, https://doi.org/10.1029/2001jd001245, 2002.

Kgope, B. S., Bond, W. J., and Midgley, G. F.: Growth responses of African savanna trees implicate atmospheric [CO2] as a driver of past and current changes in savanna tree cover, Austral Ecology, 35, 451–463, 2010.

Kirschbaum, M. U. F.: Direct and indirect climate change effects on photosynthesis and transpiration, Plant Biology, 6, 242–253, https://doi.org/10.1055/s-2004-820883, 2004.

Kumar, D. and Scheiter, S.: Biome diversity in South Asia-How can we improve vegetation models to understand global change impact at regional level?, Science of The Total Environment, 671, 1001–1016, https://doi.org/10.1016/j.scitotenv.2019.03.251, 2019.

Kumar, D., Pfeiffer, M., Gaillard, C., Langan, L., Martens, C., and Scheiter, S.: Misinterpretation of Asian savannas as degraded forest can mislead management and conservation policy under climate change, Biological Conservation, 241, 108 293, https://doi.org/10.1016/j.biocon.2019.108293, 2020.

Kumar, R. S.: A review of biodiversity studies of soil dwelling organisms in Indian mangroves, Zoos' Print Journal, 15, 221–227, https://doi.org/10.11609/jott.zpj.15.3.221-7, 2000.

Körner, C.: Paradigm shift in plant growth control, Current opinion in plant biology, 25, 107–114, https://doi.org/10.1016/j.pbi.2015.05.003, publisher: Elsevier, 2015.

Körner, C., Asshoff, R., Bignucolo, O., Hättenschwiler, S., Keel, S. G., Peláez-Riedl, S., Pepin, S., Siegwolf, R. T., and Zotz, G.: Carbon flux and growth in mature deciduous forest trees exposed to elevated CO2, Science, 309, 1360–1362, 2005.

Langan, L., Higgins, S. I., and Scheiter, S.: Climate-biomes, pedo-biomes or pyro-biomes: which world view explains the tropical forest–savanna boundary in South America?, Journal of Biogeography, 44, 2319–2330, https://doi.org/10.1111/jbi.13018, 2017.

Lapola, D. M., Priess, J. A., and Bondeau, A.: Modeling the land requirements and potential productivity of sugarcane and jatropha in Brazil and India using the LPJmL dynamic global vegetation model, Biomass and Bioenergy, 33, 1087–1095, https://doi.org/10.1016/j.biombioe.2009.04.005, 2009.

Leakey, A. D., Ainsworth, E. A., Bernacchi, C. J., Rogers, A., Long, S. P., and Ort, D. R.: Elevated CO_2 effects on plant carbon, nitrogen, and water relations: six important lessons from FACE, Journal of experimental botany, 60, 2859–2876, https://doi.org/10.1093/jxb/erp096, 2009.

Liu, M., Tian, H., Chen, G., Ren, W., Zhang, C., and Liu, J.: Effects of Land-Use and Land-Cover Change on Evapotranspiration and Water Yield in China During 1900-2000 1, JAWRA Journal of the American Water Resources Association, 44, 1193–1207, https://doi.org/10.1111/j.1752-1688.2008.00243.x, 2008.

Liu, M.-Z. and Osborne, C. P.: Leaf cold acclimation and freezing injury in C3 and C4 grasses of the Mongolian Plateau, Journal of experimental Botany, 59, 4161–4170, https://doi.org/10.1093/jxb/ern257, 2008.

Lloyd, J., Bird, M. I., Vellen, L., Miranda, A. C., Veenendaal, E. M., Djagbletey, G., Miranda, H. S., Cook, G., and Farquhar, G. D.: Contributions of woody and herbaceous vegetation to tropical savanna ecosystem productivity: a quasi-global estimate, Tree physiology, 28, 451–468, https://doi.org/10.1093/treephys/28.3.451, 2008.

Lombardozzi, D. L., Bonan, G. B., Smith, N. G., Dukes, J. S., and Fisher, R. A.: Temperature acclimation of photosynthesis and respiration: A key uncertainty in the carbon cycle-climate feedback, Geophysical Research Letters, 42, 8624–8631, https://doi.org/10.1002/2015gl065934, publisher: Wiley Online Library, 2015.

Long, S. P., Ainsworth, E. A., Rogers, A., and Ort, D. R.: Rising atmospheric carbon dioxide: plants FACE the future, Annu. Rev. Plant Biol., 55, 591–628, https://doi.org/10.1146/annurev.arplant.55.031903.141610, 2004.

Loreau, M., Naeem, S., Inchausti, P., Bengtsson, J., Grime, J. P., Hector, A., Hooper, D. U., Huston, M. A., Raffaelli, D., and Schmid, B.: Biodiversity and ecosystem functioning: current knowledge and future challenges, science, 294, 804–808, https://doi.org/10.1126/science.1064088, 2001.

Mao, J., Fu, W., Shi, X., Ricciuto, D. M., Fisher, J. B., Dickinson, R. E., Wei, Y., Shem, W., Piao, S., and Wang, K.: Disentangling climatic and anthropogenic controls on global terrestrial evapotranspiration trends, Environmental Research Letters, 10, 094 008, https://doi.org/10.1088/1748-9326/10/9/094008, 2015.

McSweeney, C. F. and Jones, R. G.: How representative is the spread of climate projections from the 5 CMIP5 GCMs used in ISI-MIP?, Climate Services, 1, 24–29, https://doi.org/10.1016/j.cliser.2016.02.001, publisher: Elsevier, 2016.

Meinshausen, M., Smith, S. J., Calvin, K., Daniel, J. S., Kainuma, M. L. T., Lamarque, J.-F., Matsumoto, K., Montzka, S. A., Raper, S. C. B., and Riahi, K.: The RCP greenhouse gas concentrations and their extensions from 1765 to 2300, Climatic change, 109, 213, https://doi.org/10.1007/s10584-011-0156-z, 2011.

Myers, N., Mittermeier, R. A., Mittermeier, C. G., Da Fonseca, G. A., and Kent, J.: Biodiversity hotspots for conservation priorities, Nature, 403, 853, https://doi.org/10.1038/35002501, 2000.

Nachtergaele, F., van Velthuizen, H., Verelst, L., Batjes, N., Dijkshoorn, K., Van Engelen, V., Fischer, G., Jones, A., Montanarella, L., and Petri, M.: Harmonized world soil database (version 1.1), FAO, Rome, Italy & IIASA, Laxenburg, Austria, 2009.

Nolan, C., Overpeck, J. T., Allen, J. R., Anderson, P. M., Betancourt, J. L., Binney, H. A., Brewer, S., Bush, M. B., Chase, B. M., and Cheddadi, R.: Past and future global transformation of terrestrial ecosystems under climate change, Science, 361, 920–923, https://doi.org/10.1126/science.aan5360, 2018.

640 Norby, R. J. and Zak, D. R.: Ecological lessons from free-air CO2 enrichment (FACE) experiments, Annual review of ecology, evolution, and systematics, 42, 181–203, https://doi.org/10.1146/annurev-ecolsys-102209-144647, 2011.

Overpeck, J. T., Rind, D., and Goldberg, R.: Climate-induced changes in forest disturbance and vegetation, Nature, 343, 51, https://doi.org/10.1038/343051a0, 1990.

Parr, C. L., Gray, E. F., and Bond, W. J.: Cascading biodiversity and functional consequences of a global change–induced biome switch, 645 Diversity and Distributions, 18, 493–503, https://doi.org/10.1111/j.1472-4642.2012.00882.x, 2012.

Parr, C. L., Lehmann, C. E., Bond, W. J., Hoffmann, W. A., and Andersen, A. N.: Tropical grassy biomes: misunderstood, neglected, and under threat, Trends in ecology & evolution, 29, 205–213, https://doi.org/10.1016/j.tree.2014.02.004, 2014.

Parry, M., Parry, M. L., Canziani, O., Palutikof, J., Van der Linden, P., and Hanson, C.: Climate change 2007-impacts, adaptation and vulnerability: Working group II contribution to the fourth assessment report of the IPCC, vol. 4, Cambridge University Press, 2007.

650 Pfeiffer, M., Langan, L., Linstädter, A., Martens, C., Gaillard, C., Ruppert, J. C., Higgins, S. I., Mudongo, E. I., and Scheiter, S.: Grazing and aridity reduce perennial grass abundance in semi-arid rangelands–Insights from a trait-based dynamic vegetation model, Ecological Modelling, 395, 11–22, https://doi.org/10.1016/j.ecolmodel.2018.12.013, 2019.

Piao, S., Friedlingstein, P., Ciais, P., Zhou, L., and Chen, A.: Effect of climate and CO2 changes on the greening of the Northern Hemisphere over the past two decades, Geophysical Research Letters, 33, https://doi.org/10.1029/2006gl028205, publisher: Wiley Online Library, 655 2006.

Prentice, I. C., Bondeau, A., Cramer, W., Harrison, S. P., Hickler, T., Lucht, W., Sitch, S., Smith, B., and Sykes, M. T.: Dynamic global vegetation modeling: quantifying terrestrial ecosystem responses to large-scale environmental change, in: Terrestrial ecosystems in a changing world, pp. 175–192, Springer, 2007.

Proença, V., Martin, L. J., Pereira, H. M., Fernandez, M., McRae, L., Belnap, J., Böhm, M., Brummitt, N., García-Moreno, J., and Gregory, 660 R. D.: Global biodiversity monitoring: from data sources to essential biodiversity variables, Biological Conservation, 213, 256–263, https://doi.org/10.1016/j.biocon.2016.07.014, 2017.

Quade, J., Cater, J. M., Ojha, T. P., Adam, J., and Mark Harrison, T.: Late Miocene environmental change in Nepal and the northern Indian subcontinent: Stable isotopic evidence from paleosols, Geological Society of America Bulletin, 107, 1381–1397, https://doi.org/10.1130/0016-7606(1995)107<1381:lmecin>2.3.co;2, 1995.

665 Ramankutty, N., Foley, J. A., Hall, F., Collatz, G., Meeson, B., LOS, S., Brown DE Colstoun, E., and Landis, D.: ISLSCP II Potential Natural Vegetation Cover, ORNL DAAC, https://doi.org/10.3334/ornldaac/961, 2010.

Ratnam, J., Tomlinson, K. W., Rasquinha, D. N., and Sankaran, M.: Savannahs of Asia: antiquity, biogeography, and an uncertain future, Philosophical Transactions of the Royal Society B: Biological Sciences, 371, 20150 305, https://doi.org/10.1098/rstb.2015.0305, 2016.

Ravindranath, N. H., Somashekhar, B. S., and Gadgil, M.: Carbon flow in Indian forests, Climatic Change, 35, 297–320, http://repository. 670 ias.ac.in/64101/, 1997.

Ravindranath, N. H., Murali, K. S., and Sudha, P.: Community forestry initiatives in Southeast Asia: a review of ecological impacts, International Journal of Environment and Sustainable Development, 5, 1–11, https://doi.org/10.1504/ijesd.2006.008678, 2006.

Richardson, A. D., Keenan, T. F., Migliavacca, M., Ryu, Y., Sonnentag, O., and Toomey, M.: Climate change, phenology, and phenological control of vegetation feedbacks to the climate system, Agricultural and Forest Meteorology, 169, 156–173, https://doi.org/10.1016/j.agrformet.2012.09.012, publisher: Elsevier, 2013.

Ricklefs, R. E.: The economy of nature, Macmillan, 2008.

Rodgers, W. A. and Panwar, H. S.: Planning a wildlife protected area network in India, 1988.

Saatchi, S. S., Harris, N. L., Brown, S., Lefsky, M., Mitchard, E. T., Salas, W., Zutta, B. R., Buermann, W., Lewis, S. L., and Hagen, S.: Benchmark map of forest carbon stocks in tropical regions across three continents, Proceedings of the national academy of sciences, 108, 9899–9904, https://doi.org/10.1073/pnas.1019576108, 2011.

Saikia, P., Deka, J., Bharali, S., Kumar, A., Tripathi, O. P., Singha, L. B., Dayanandan, S., and Khan, M. L.: Plant diversity patterns and conservation status of eastern Himalayan forests in Arunachal Pradesh, Northeast India, Forest Ecosystems, 4, 28, https://doi.org/10.1186/s40663-017-0117-8, publisher: Springer, 2017.

Sakschewski, B., Bloh, W., Boit, A., Rammig, A., Kattge, J., Poorter, L., Peñuelas, J., and Thonicke, K.: Leaf and stem economics spectra drive diversity of functional plant traits in a dynamic global vegetation model, Global Change Biology, 21, 2711–2725, https://doi.org/10.1111/gcb.12870, 2015.

Sato, H., Itoh, A., and Kohyama, T.: SEIB–DGVM: A new Dynamic Global Vegetation Model using a spatially explicit individual-based approach, Ecological Modelling, 200, 279–307, https://doi.org/10.1016/j.ecolmodel.2006.09.006, publisher: Elsevier, 2007.

Scheiter, S., Langan, L., and Higgins, S. I.: Next-generation dynamic global vegetation models: learning from community ecology, New Phytologist, 198, 957–969, https://doi.org/10.1111/nph.12210, 2013.

Schimel, D., Stephens, B. B., and Fisher, J. B.: Effect of increasing CO2 on the terrestrial carbon cycle, Proceedings of the National Academy of Sciences, 112, 436–441, https://doi.org/10.1073/pnas.1407302112, publisher: National Acad Sciences, 2015.

Sharkey, T. D., Bernacchi, C. J., Farquhar, G. D., and Singsaas, E. L.: Fitting photosynthetic carbon dioxide response curves for C3 leaves, Plant, cell & environment, 30, 1035–1040, https://doi.org/10.1111/j.1365-3040.2007.01710.x, 2007.

Simard, M., Pinto, N., Fisher, J. B., and Baccini, A.: Mapping forest canopy height globally with spaceborne lidar, Journal of Geophysical Research: Biogeosciences, 116, https://doi.org/10.1029/2011jg001708, 2011.

Sinha, S., Badola, H. K., Chhetri, B., Gaira, K. S., Lepcha, J., and Dhyani, P. P.: Effect of altitude and climate in shaping the forest compositions of Singalila National Park in Khangchendzonga Landscape, Eastern Himalaya, India, Journal of Asia-Pacific Biodiversity, 11, 267–275, https://doi.org/10.1016/j.japb.2018.01.012, 2018.

Smith, B., Wårlind, D., Arneth, A., Hickler, T., Leadley, P., Siltberg, J., and Zaehle, S.: Implications of incorporating N cycling and N limitations on primary production in an individual-based dynamic vegetation model, pp. 18 613–18 685, https://doi.org/10.5194/bgd-10-18613-2013.

Soh, W. K., Yiotis, C., Murray, M., Parnell, A., Wright, I. J., Spicer, R. A., Lawson, T., Caballero, R., and McElwain, J. C.: Rising CO2 drives divergence in water use efficiency of evergreen and deciduous plants, Science Advances, 5, eaax7906, https://doi.org/10.1126/sciadv.aax7906, 2019.

Stephenson, N.: Actual evapotranspiration and deficit: biologically meaningful correlates of vegetation distribution across spatial scales, Journal of Biogeography, 25, 855–870, https://doi.org/10.1046/j.1365-2699.1998.00233.x, 1998.

Stevens, N., Lehmann, C. E., Murphy, B. P., and Durigan, G.: Savanna woody encroachment is widespread across three continents, Global change biology, 23, 235–244, https://doi.org/10.1111/gcb.13409, 2017.

710   Terrer, C., Vicca, S., Stocker, B. D., Hungate, B. A., Phillips, R. P., Reich, P. B., Finzi, A. C., and Prentice, I. C.: Ecosystem responses to elevated CO 2 governed by plant–soil interactions and the cost of nitrogen acquisition, New Phytologist, 217, 507–522, https://doi.org/10.1111/nph.14872, 2018.

Thuiller, W., Albert, C., Araújo, M. B., Berry, P. M., Cabeza, M., Guisan, A., Hickler, T., Midgley, G. F., Paterson, J., Schurr, F. M., and others: Predicting global change impacts on plant species' distributions: future challenges, Perspectives in Plant Ecology, Evolution and
715   Systematics, 9, 137–152, https://doi.org/10.1016/j.ppees.2007.09.004, 2008.

Torello-Raventos, M., Feldpausch, T. R., Veenendaal, E., Schrodt, F., Saiz, G., Domingues, T. F., Djagbletey, G., Ford, A., Kemp, J., and Marimon, B. S.: On the delineation of tropical vegetation types with an emphasis on forest/savanna transitions, Plant Ecology & Diversity, 6, 101–137, https://doi.org/10.1080/17550874.2012.762812, 2013.

Tuanmu, M.-N. and Jetz, W.: A global 1-km consensus land-cover product for biodiversity and ecosystem modelling, Global Ecology and
720   Biogeography, 23, 1031–1045, https://doi.org/10.1111/geb.12182, 2014.

Urban, J., Ingwers, M., McGuire, M. A., and Teskey, R. O.: Stomatal conductance increases with rising temperature, Plant signaling & behavior, 12, e1356 534, https://doi.org/10.1080/15592324.2017.1356534, 2017.

Van Vuuren, D. P., Edmonds, J., Kainuma, M., Riahi, K., Thomson, A., Hibbard, K., Hurtt, G. C., Kram, T., Krey, V., and Lamarque, J.-F.: The representative concentration pathways: an overview, Climatic change, 109, 5, https://doi.org/10.1007/s10584-011-0148-z, 2011.

725   Verstraete, M. M., Scholes, R. J., and Smith, M. S.: Climate and desertification: looking at an old problem through new lenses, Frontiers in Ecology and the Environment, 7, 421–428, https://doi.org/10.1890/080119, 2009.

Wang, X., Wang, T., Liu, D., Guo, H., Huang, H., and Zhao, Y.: Moisture-induced greening of the South Asia over the past three decades, Global change biology, 23, 4995–5005, https://doi.org/10.1111/gcb.13762, 2017.

Warren, J. M., Pötzelsberger, E., Wullschleger, S. D., Thornton, P. E., Hasenauer, H., and Norby, R. J.: Ecohydrologic impact of reduced
730   stomatal conductance in forests exposed to elevated CO2, Ecohydrology, 4, 196–210, 2011.

Warszawski, L., Frieler, K., Huber, V., Piontek, F., Serdeczny, O., and Schewe, J.: The inter-sectoral impact model intercomparison project (ISI–MIP): project framework, Proceedings of the National Academy of Sciences, 111, 3228–3232, 2014.

Whittaker, R. H.: Dominance-types, Classification of plant communities, pp. 65–79, https://doi.org/10.1007/978-94-009-9183-5_3, 1978.

Wingfield, J. C.: Ecological processes and the ecology of stress: the impacts of abiotic environmental factors, Functional Ecology, 27, 37–44,
735   https://doi.org/10.1111/1365-2435.12039, 2013.

Zemunik, G., Turner, B. L., Lambers, H., and Laliberté, E.: Diversity of plant nutrient-acquisition strategies increases during long-term ecosystem development, Nature plants, 1, 15 050, https://doi.org/10.1038/nplants.2015.50, 2015.

Zhang, K., Kimball, J. S., Nemani, R. R., and Running, S. W.: A continuous satellite-derived global record of land surface evapotranspiration from 1983 to 2006, Water Resources Research, 46, https://doi.org/10.1029/2009wr008800, 2010.

740   Zhang, Y., Peña-Arancibia, J. L., McVicar, T. R., Chiew, F. H., Vaze, J., Liu, C., Lu, X., Zheng, H., Wang, Y., and Liu, Y. Y.: Multi-decadal trends in global terrestrial evapotranspiration and its components, Scientific reports, 6, 19 124, https://doi.org/10.1038/srep19124, 2016.

Table 1. Biome cover (in %) for the 2000s, 2050s and 2090s, and percent (%) change in biome cover from the 2000s to 2050s and the 2000s to 2090s under RCP4.5 and RCP8.5 with fixed and elevated CO2. Δ indicates percentual biomass changes between time periods.

RCP Scenarios	Year	Barren	C$_4$ Grassland	C$_3$ Grassland	Woodland	Evg. forest	Dec. forest	Shrubland	C$_4$ Savanna	C$_3$ Savanna
	2010s	5.6	15.4	4.6	18.2	11.7	17.6	6.9	17.7	2.4
RCP4.5 + fCO2	2050s	6.3	14.8	3.2	15.7	11.2	18.6	6.7	22.1	1.4
	2090s	10.4	12.3	2.3	10.0	12.7	20.1	6.0	24.7	1.4
	Δ 2050s-2010s	13.0	-3.7	-32.2	-13.6	-4.0	5.6	-3.0	25.4	-39.1
	Δ 2090s-2010s	87.0	-20.1	-50.0	-45.2	7.9	14.4	-12.7	40.1	-41.3
	2010s	5.7	15.2	4.8	18.6	11.5	17.5	6.8	17.5	2.4
	2050s	6.5	13.9	3.5	15.0	11.9	21.2	7.0	19.6	1.3
RCP4.5+ eCO2	2090s	10.4	10.4	2.5	10.7	15.9	27.9	6.2	15.1	0.9
	Δ 2050s-2010s	13.5	-8.2	-26.9	-19.7	3.1	21.2	3.8	12.1	-44.7
	Δ 2090s-2010s	82.0	-31.6	-48.4	-42.4	38.0	59.1	-8.4	-14.1	-63.8
	2010s	6.3	14.7	4.5	18.8	11.7	17.3	6.3	18.0	2.4
	2050s	8.8	12.3	2.5	14.7	12.9	21.7	6.6	19.0	1.5
RCP8.5 + fCO2	2090s	9.4	15.0	2.5	11.0	10.8	14.2	6.7	29.0	1.4
	Δ 2050s-2010s	39.0	-16.5	-43.7	-21.9	10.1	25.0	4.1	5.4	-39.1
	Δ 2090s-2010s	48.8	1.8	-43.7	-41.6	-7.9	-17.9	5.7	61.0	-41.3
	2010s	5.9	14.8	4.7	18.0	11.6	17.5	7.1	17.9	2.5
	2050s	9.7	10.5	3.2	13.9	14.5	25.4	7.1	14.1	1.6
RCP8.5 + eCO2	2090s	6.3	11.5	4.2	12.6	17.0	28.0	7.0	12.2	1.3
	Δ 2050s-2010s	64.9	-29.5	-32.6	-22.9	24.8	45.4	0.7	-21.6	-35.4
	Δ 2090s-2010s	7.0	-22.2	-10.9	-30.3	46.5	60.2	-1.5	-32.2	-47.9

Table 2. Mean biomass (in t/ha) within biomes for the 2000s, 2050s and 2090s, and percent (%) change in biomass from the 2000s to 2050s and the 2000s to 2090s under RCP4.5 and RCP8.5 with fixed and elevated CO2. Δ indicates percentual biomass changes between time periods.

RCP Scenarios	Year	C$_4$ Grassland	C$_3$ Grassland	Woodland	Evg. forest	Dec. forest	Shrubland	C$_4$ Savanna	C$_3$ Savanna
RCP4.5 + fCO2	2010s	0.9	1.5	30.4	189.7	142.1	4.0	35.5	36.8
	2050s	0.9	1.8	29.2	191.0	144.0	3.6	38.0	44.7
	2090s	0.9	2.1	24.5	188.1	148.4	3.3	32.6	31.8
	Δ 2050s-2010s	-1.1	19.5	-4.0	0.7	1.3	-10.9	6.8	21.4
	Δ 2090s-2010s	4.4	35.1	-19.4	-0.9	4.4	-17.8	-8.2	-13.7
RCP4.5 + eCO2	2010s	0.9	1.4	30.7	189.2	142.5	4.0	35.9	37.3
	2050s	1.0	1.5	34.7	204.6	162.9	4.3	48.1	53.2
	2090s	1.0	1.6	29.3	196.4	164.9	4.1	43.2	51.8
	Δ 2050s-2010s	17.2	5.6	13.0	8.1	14.4	6.0	34.0	42.7
	Δ 2090s-2010s	12.6	8.3	-4.6	3.8	15.7	2.5	20.4	39.1
RCP8.5 + fCO2	2010s	0.9	1.5	30.7	191.1	146.3	3.9	35.8	34.9
	2050s	0.7	1.6	23.5	182.1	134.7	3.3	31.2	28.0
	2090s	0.8	1.6	18.7	175.7	136.4	3.1	28.5	33.2
	Δ 2050s-2010s	-19.1	4.7	-23.4	-4.7	-7.9	-15.3	-12.8	-19.7
	Δ 2090s-2010s	-14.6	4.7	-39.0	-8.0	-6.8	-20.0	-20.5	-4.9
RCP8.5 + eCO2	2010s	0.9	1.3	31.2	188.3	146.1	4.1	36.5	32.0
	2050s	1.0	1.4	32.1	206.3	162.7	4.0	45.1	47.2
	2090s	0.7	1.1	30.8	206.0	183.4	4.7	49.8	50.7
	Δ 2050s-2010s	9.9	8.7	2.8	9.6	11.3	-1.5	23.6	47.4
	Δ 2090s-2010s	-22.0	-12.7	-1.6	9.4	25.6	15.5	36.6	58.2

Table 3. Biome-level ET normalized to biomass (Ebiomes, mm/kg/year) for the 2000s, 2050s and 2090s, and percent (%) change in Ebiomes from the 2000s to 2050s and the 2000s to 2090s under RCP4.5 and RCP8.5 with fixed and elevated CO2. Δ indicates percentual ET changes between time periods.

RCP Scenarios	Year	C₄ Grassland	C₃ Grassland	Woodland	Evg. forest	Dec. forest	Shrubland	C₄ Savanna	C₃ Savanna
	2010s	186.7	95.5	257	159.7	288.5	183.3	252.5	194.2
	2050s	170.9	80.5	217	157.4	291.3	187.2	244.6	151.9
RCP4.5 + fCO2	2090s	185	72.3	209.6	140.7	289.3	205.2	247.1	179.1
	Δ 2050s-2010s	-8.5	-15.7	-15.6	-1.4	1	2.1	-3.1	-21.8
	Δ 2090s-2010s	-0.9	-24.3	-18.5	-11.9	0.3	11.9	-2.1	-7.8
	2010s	185.4	93.4	259.7	159.7	288.1	190.9	251.6	188.4
	2050s	161.2	79.7	217	147.8	283	183.2	238.2	153.4
RCP4.5 + eCO2	2090s	164.1	73.4	210.2	138.7	280.4	197.2	236.6	157.1
	Δ 2050s-2010s	-13.1	-14.6	-16.5	-7.4	-1.8	-4.1	-5.3	-18.6
	Δ 2090s-2010s	-11.5	-21.4	-19.1	-13.2	-2.7	3.3	-6	-16.6
	2010s	172.8	87.4	257.5	160.9	286.5	185.5	244.7	188.1
	2050s	153.7	72.7	243.2	158.3	298.5	195.1	241	162.7
RCP8.5 + fCO2	2090s	195.6	67.6	231.1	162.7	301.3	216	267.5	150.2
	Δ 2050s-2010s	-11.1	-16.8	-5.5	-1.6	4.2	5.2	-1.5	-13.5
	Δ 2090s-2010s	13.2	-22.6	-10.2	1.1	5.2	16.4	9.3	-20.1
	2010s	177.5	91.1	256.4	162.7	284.5	192.5	243.7	191.7
	2050s	143.9	76.9	235.6	149.4	285.4	184.6	228.8	153.1
RCP8.5 + eCO2	2090s	141.4	59.2	218.3	143.9	284.9	186	242.3	143.2
	Δ 2050s-2010s	-18.9	-15.6	-8.1	-8.1	0.3	-4.1	-6.1	-20.1
	Δ 2090s-2010s	-20.3	-35.1	-14.9	-11.6	0.1	-3.4	-0.6	-25.3
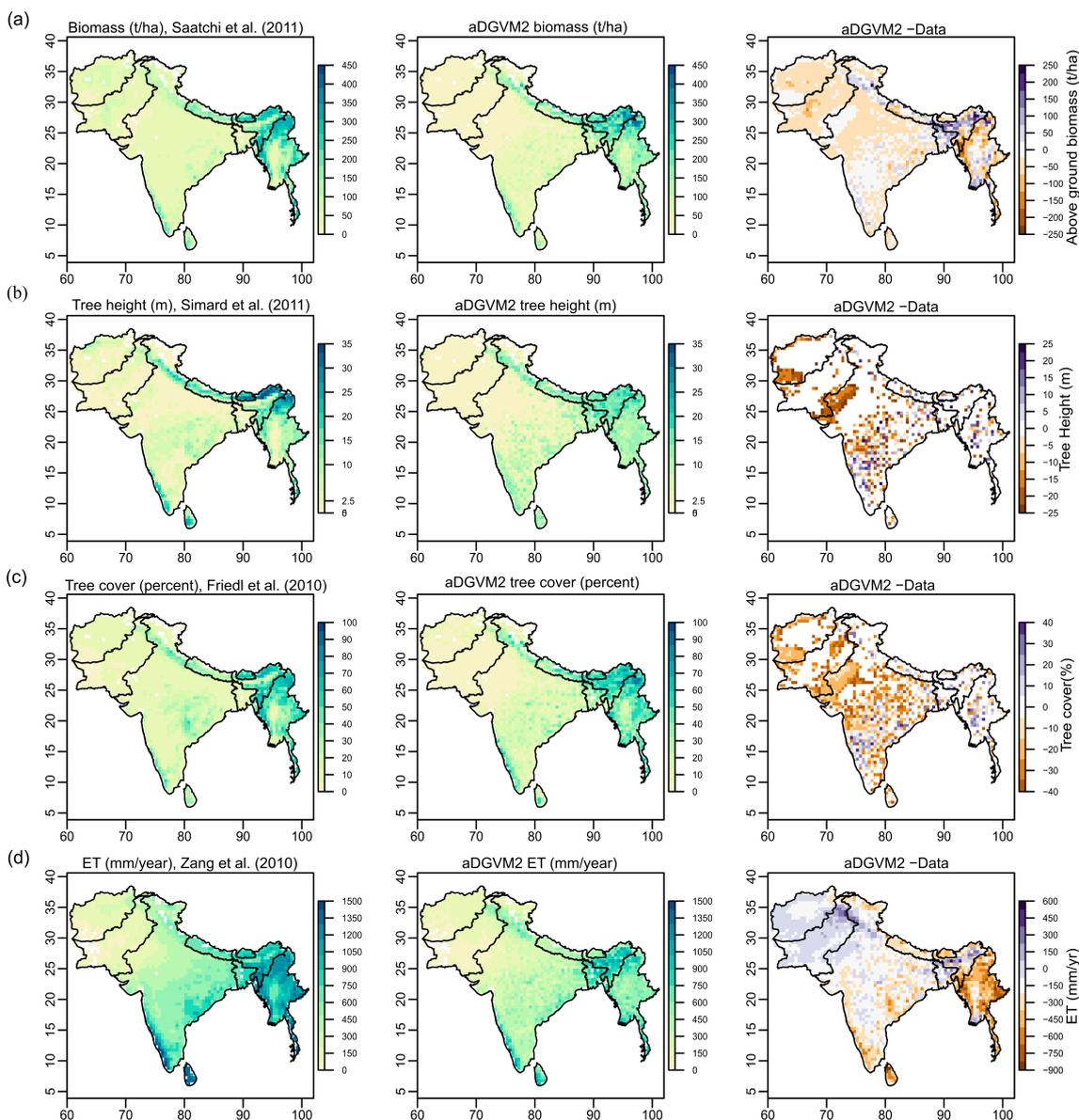
Figure 1. : Comparison between aDGVM2 results and data for (a) simulated biomass and Saatchi et al. (2011) biomass and their difference, (b) simulated tree height and Simard et al. (2011) and their difference, (c) simulated tree cover and Friedl et al. (2011) tree cover and their difference and (d) simulated evapotranspiration and Zang et al. (2010) evapotranspiration and their difference. In the figure the first column shows the remote sensing products, the second column shows aDGVM2 results, and the third column shows the difference between simulation and data. For results with masked land use cover see supplementary Figure S2.
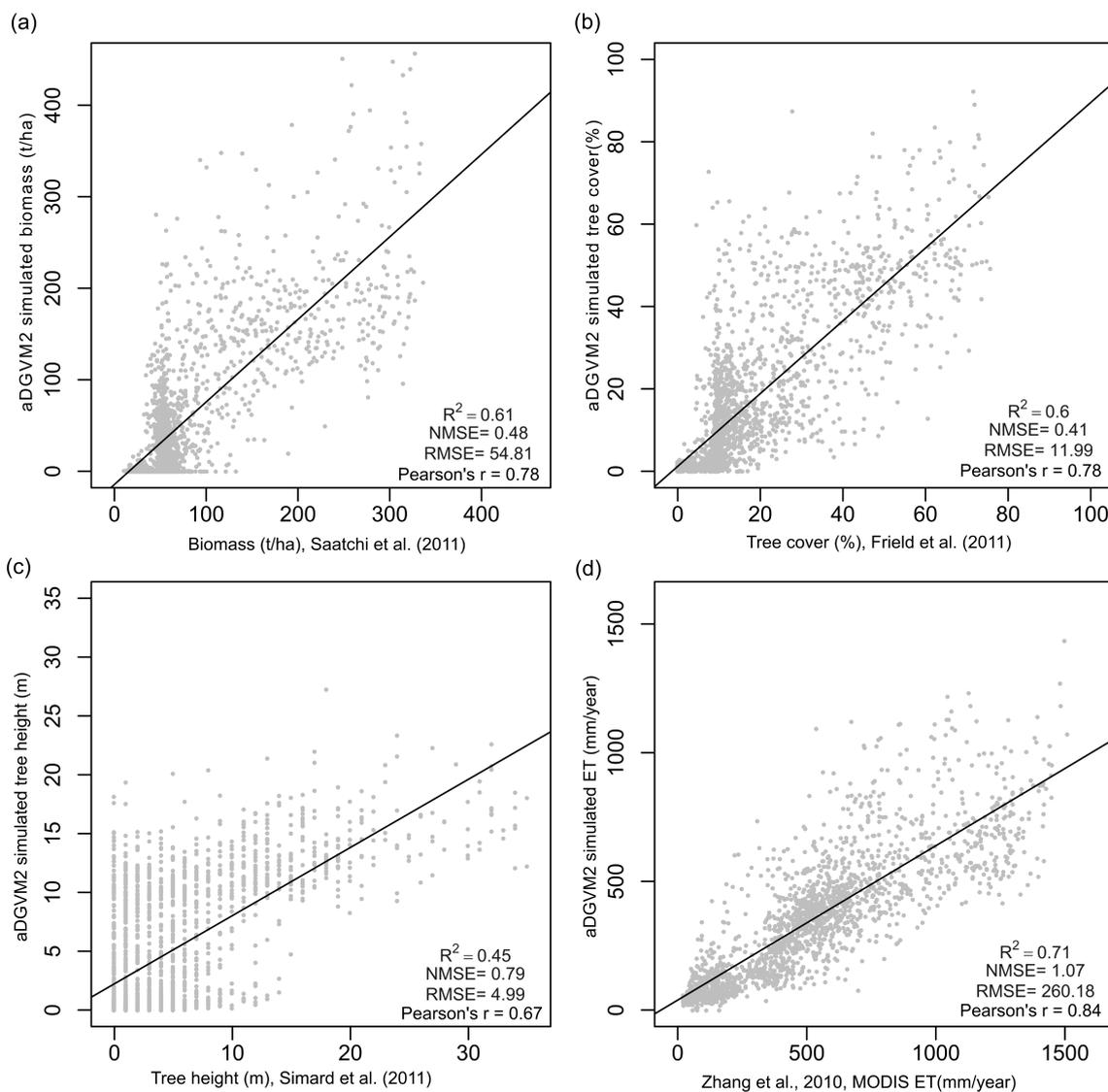
Figure 2. Scatterplots for simulated state variables against benchmarking data. (a) Simulated biomass and Saatchi et al. (2011) biomass, (b) simulated tree cover and Friedl et al. (2010) tree cover, (c) simulated tree height and Simard et al. (2011) tree height, and (d) simulated evapotranspiration and MODIS ET (Zhang et al., 2010). NMSE and RMSE are normalized mean square error and root mean square error, respectively. Each point represents one grid cell in the study region.
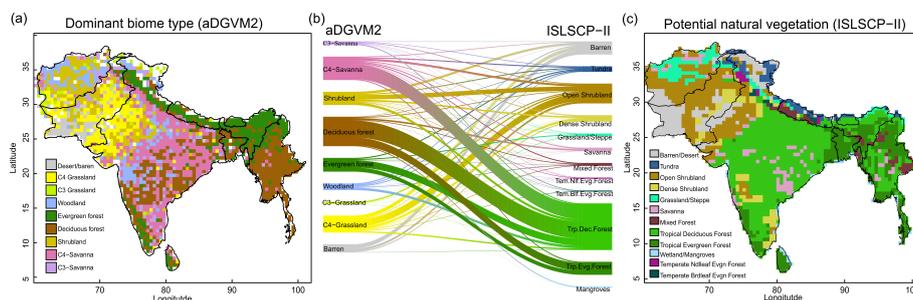
Figure 3. Comparison between simulated and observed biome patterns. (a) Simulated dominant biome type, (b) Sankey diagram showing overlap between simulated biomes and potential natural vegetation cover (ISLSCP-II, Ramankutty et al., 2010) and (c) potential natural vegetation. The Sankey graph shows how aDGVM2 biomes and PNV classes overlap.
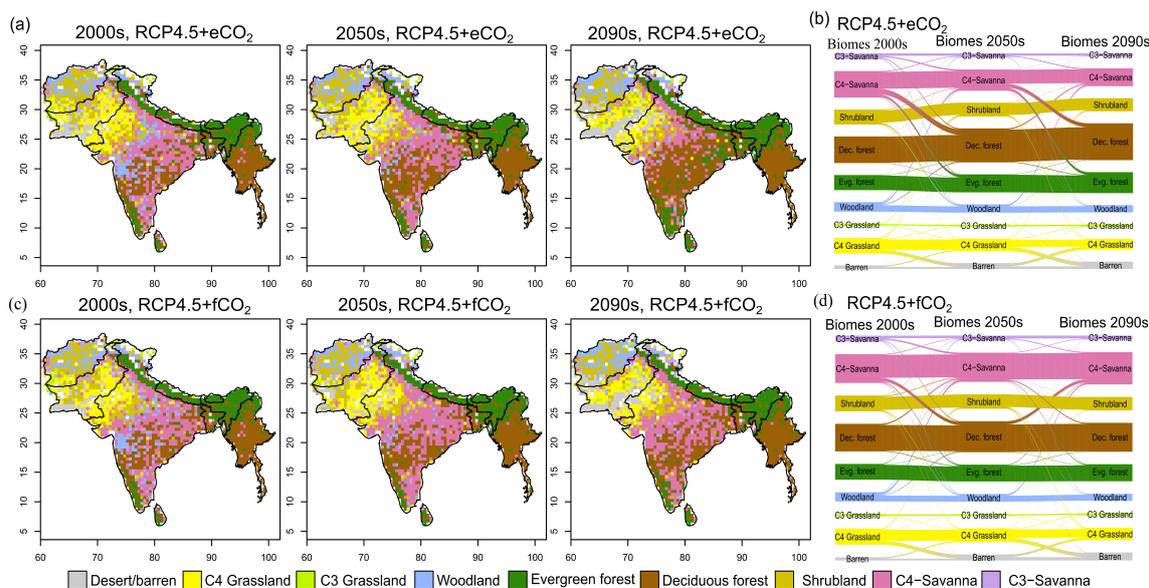
Figure 4. Simulated biome distribution for the 2000s, 2050s and 2090s under (a) RCP4.5+eCO$_2$ and (c) RCP4.5+fCO$_2$, and Sankey diagrams showing the fractional cover of biomes and transitions between biomes from the 2000s to the 2050s and the 2050s to the 2090s under (b) RCP4.5+eCO$_2$ and (d) RCP4.5+fCO$_2$. See Figure S6 for simulated biome distribution under RCP8.5.
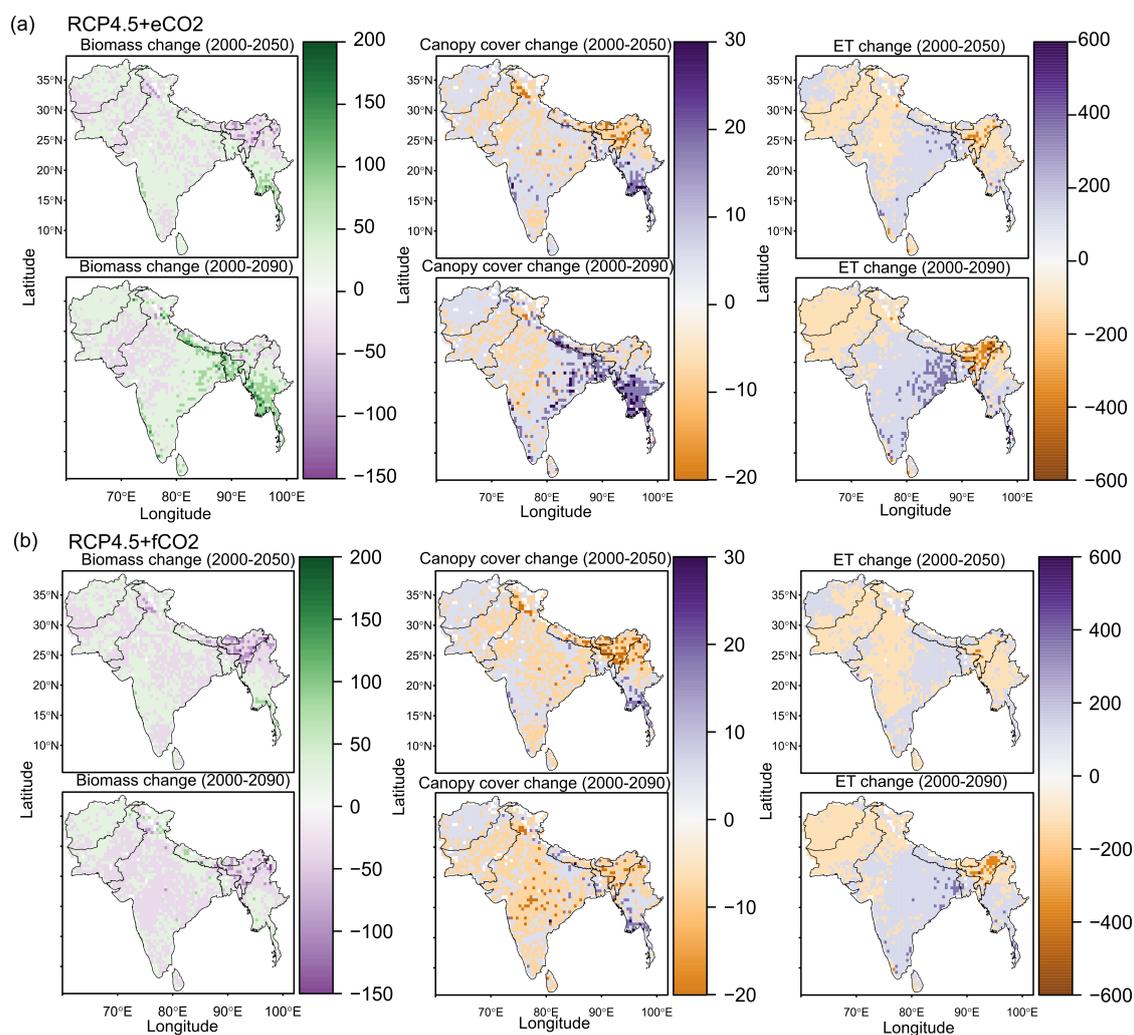
Figure 5. Projected change in biomass (t/ha), canopy area (%) and ET (mm/year) between the 2000s and 2050s, and between the 2000s and 2090s under (a) RCP4.5+eCO$_2$ and (b) RCP4.5+fCO$_2$. See Figure S7 for projected change of these variables under RCP8.5.
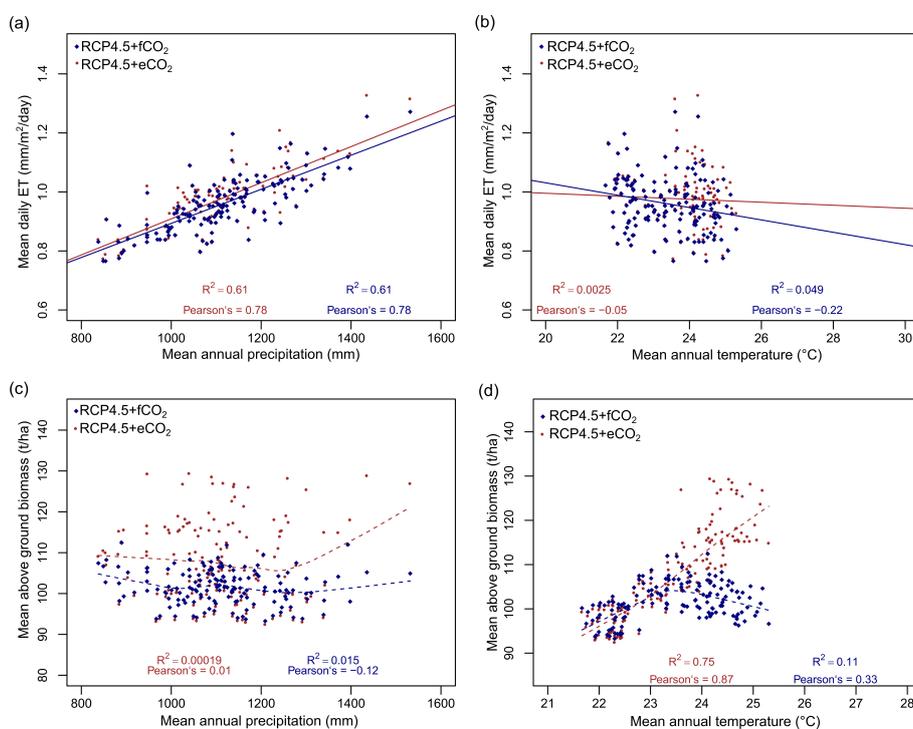
Figure 6. Relationship between (a) evapotranspiration (ET) and mean annual precipitation (MAP), (b) ET and mean annual temperature (MAT), (c) mean above ground biomass and MAP and (d) mean above ground biomass and MAT under RCP4.5. The lines (both solid and dotted) in all figures represent the best-fit regression line. Data points represent spatially averaged ET (a, b) and biomass (c, d) for each year from 1950 to 2099. See Figure S8 for these relation between ET, biomass, MAP and MAT under RCP8.5.
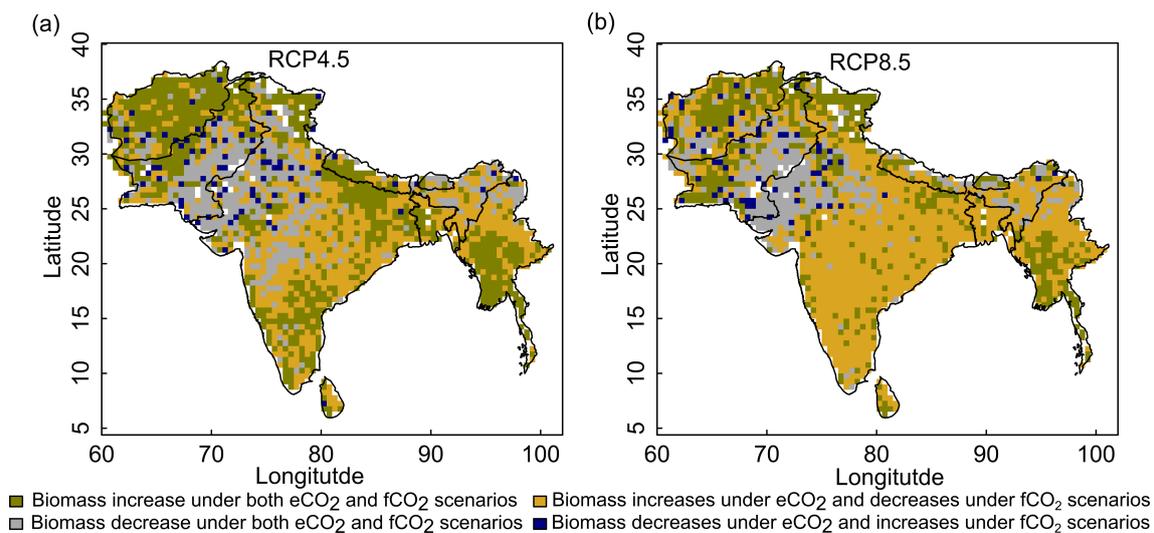
Figure 7. Maps showing areas where CO_2-fertilization compensates biomass dieback caused by climate change between 2000s and 2090s under (a) RCP4.5 and (b) RCP8.5.
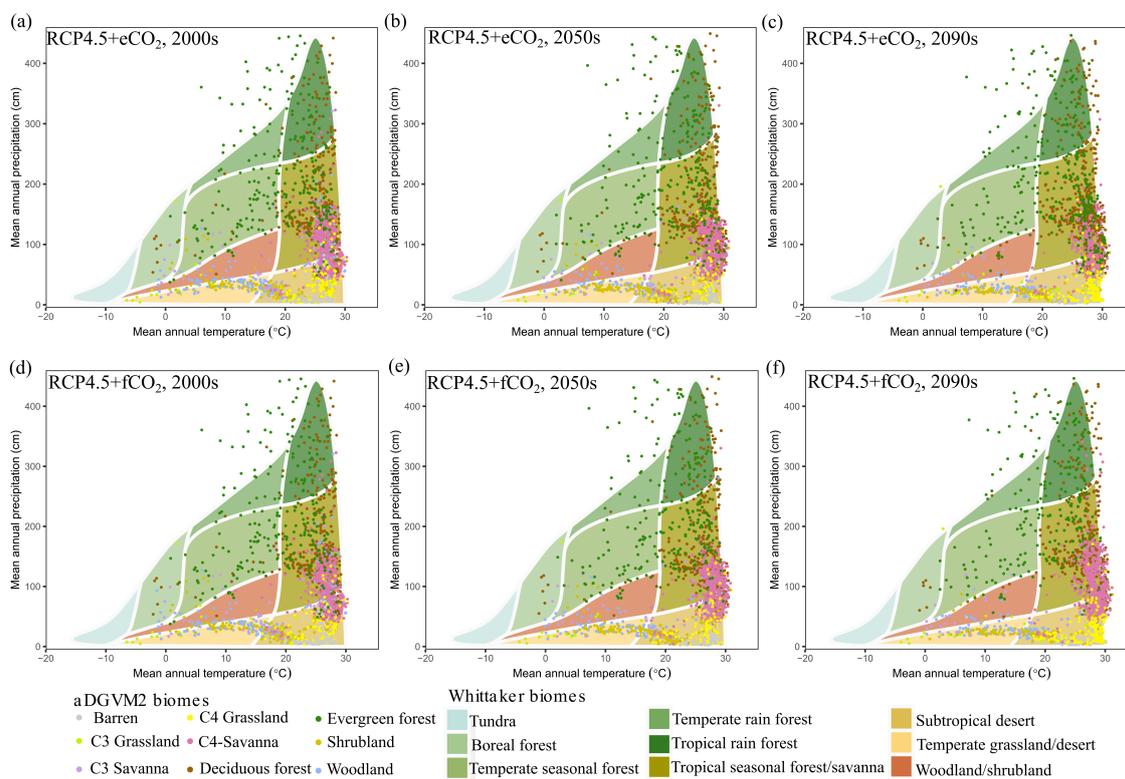
Figure 8. Simulated climate niches of biomes for the (a) 2000s, (b) 2050s and (c) 2090s under RCP4.5+eCO$_2$ and (d) 2000s, (e) 2050s and (f) 2090s under RCP4.5+fCO$_2$. The simulated biomes are overlaid on the climate envelopes of Whittaker's biomes and are plotted following Ricklefs (2008) and Whittaker (1975). See Figure S9 for projected change in climatic niches of biomes under RCP8.5.